

2016

# Electrophysiological analysis of transcranial direct current stimulation and its effect on cortical spreading depression

---

<https://hdl.handle.net/2144/16812>

*Boston University*

BOSTON UNIVERSITY  
SCHOOL OF MEDICINE

Thesis

**ELECTROPHYSIOLOGICAL ANALYSIS OF TRANSCRANIAL DIRECT  
CURRENT STIMULATION AND ITS EFFECT ON CORTICAL SPREADING  
DEPRESSION**

by

**ANDREW STANFORD CHANG**

B.A., University of California, Berkeley, 2013

Submitted in partial fulfillment of the  
requirements for the degree of  
Master of Science

2016

© 2016 by  
ANDREW STANFORD CHANG  
All rights reserved

Approved by

First Reader

---

Richard J. Rushmore, Ph.D.  
Assistant Professor of Anatomy and Neurobiology

Second Reader

---

Theresa A. Davies, Ph.D.  
Assistant Professor of Medical Sciences and Education

## ACKNOWLEDGMENTS

Dr. Richard Jarrett Rushmore III, Ph.D.:

Good mentorship is rare and of great value. Your mentorship has been of worth beyond price. Thank you for helping me to broaden my mental horizons: to begin to think not only as a student, but also as a scientist.

Dr. Theresa A. Davies, Ph.D.:

Thank you for your helpful expertise and efficiency during the thesis review process, when time was at a great premium.

Aquina Wihak, Patrick McGillen, Alina Bazarian, and Ian Benjamin:

To say that my spirits were constantly buoyed by your presences on a journey that would otherwise have been frequently dark and lonely would be a gross understatement. Thank you for friendship, moral support, technical expertise, and scientific enthusiasm.

**ELECTROPHYSIOLOGICAL ANALYSIS OF TRANSCRANIAL DIRECT  
CURRENT STIMULATION AND ITS EFFECT ON CORTICAL SPREADING  
DEPRESSION**

**ANDREW STANFORD CHANG**

**ABSTRACT**

Transcranial direct current stimulation (TDCS) allows for the noninvasive modulation of cortical activity. In this study, the effects of cathodal and anodal TDCS treatment on baseline activity in the motor cortex of rats were investigated via translaminar electroencephalogram (EEG) recording and power spectral density analysis. Treatment with low intensity anodal TDCS for five minutes was found to increase delta and theta frequency cortical activity during and for up to five minutes following treatment.

This study also assessed the interaction of TDCS with the phenomenon of cortical spreading depression (CoSD), which has been implicated in numerous disease states, including migraine and stroke. TDCS treatment was given concurrently with induction of CoSD via administration of potassium chloride to the surface of the dura. The presence of the spreading depression event, a characteristic low frequency wave observed to travel outwards from the point of CoSD induction and downwards through the cortex, was used as a proxy measure for the occurrence of CoSD. It was observed that animals treated with cathodal TDCS exhibited fewer spreading depression events relative to those treated with anodal TDCS or those receiving sham treatment.

In this study, animals were segregated into groups that exhibited stimulus artifact during TDCS treatment and those that did not. Stimulus artifact was defined as a characteristic alpha and/or beta frequency activity spike lasting throughout and not longer than the period of stimulation. Those animals receiving TDCS without exhibiting stimulus artifact were considered for the purposes of this study to not have received proper TDCS treatment, and acted as a sham treatment group. Because salient differences emerged between the stimulus artifact positive and stimulus artifact negative groups, this study suggests that the presence of stimulus artifact could be used as a proxy measure for successful TDCS dosage.

## TABLE OF CONTENTS

TITLE .....	i
COPYRIGHT PAGE .....	ii
READER APPROVAL PAGE.....	iii
ACKNOWLEDGMENTS .....	iv
ABSTRACT.....	v
TABLE OF CONTENTS.....	vii
LIST OF TABLES .....	x
LIST OF FIGURES .....	xi
LIST OF ABBREVIATIONS.....	xiii
INTRODUCTION .....	1
Transcranial Direct Current Stimulation.....	1
Cortical Spreading Depression .....	3
Cortical Spreading Depression and Transcranial Direct Current Stimulation.....	5
AIMS AND OBJECTIVES .....	7
METHODS .....	10
Animals.....	10
Surgical Procedure .....	10



Electroencephalogram (EEG) Recording and Paired Pulse Stimulation Setup .....	12
TDCS Setup .....	12
Potassium Chloride (KCl) Drop Setup .....	13
Experimental Procedure and Data Collection.....	13
Perfusion Procedure .....	14
Analyzing the Effect of TDCS on Baseline Activity.....	15
Observing the Effect of TDCS on Cortical Spreading Depression Events.....	17
RESULTS .....	18
Experimental Setup and Data Processing .....	18
The Effect of TDCS on Baseline Cortical Activity .....	21
Segregation of Groups .....	21
Group 1: Anodal TDCS with Stimulus Artifact .....	22
Group 2: Anodal TDCS without Stimulus Artifact .....	27
Group 3: Cathodal TDCS with Stimulus Artifact.....	30
Group 4: Cathodal TDCS without Stimulus Artifact.....	31
The Effect of TDCS on Cortical Spreading Depression Events.....	37
Segregation and Refinement of Groups .....	37
Outcome Assessment .....	37
Transient Changes in Cortical Activity During CoSD Events.....	38

DISCUSSION .....	42
Anodal TDCS Amplifies Baseline Delta and Theta Band Activity.....	42
Cathodal TDCS Inhibits Occurrence of CoSD Events .....	43
The CoSD Event Occurs Concurrently with a Burst of Gamma Activity .....	43
TDCS Stimulus Artifact Presence Is a Useful Proxy for TDCS Dosage.....	43
Conclusion .....	44
APPENDIX A.....	46
APPENDIX B .....	49
REFERENCES .....	52
CURRICULUM VITAE.....	55

## LIST OF TABLES

<b>Table</b>	<b>Title</b>	<b>Page</b>
1	Results from assessment of the presence of CoSD events during the period of TDCS.	38

## LIST OF FIGURES

<b>Figure</b>	<b>Title</b>	<b>Page</b>
1	EEG and multi-unit activity recordings demonstrating characteristics of CoSD events in rats.	8
2	Schematic of parasagittal section of the rat brain demonstrating the approximate recording electrode placement.	18
3A	Power spectral density representation of a single recording.	19
3B	Plot displaying change in average normalized power over multiple recordings for a particular frequency band and treatment group for a single channel.	19
4	Plot of spectrogram data from MTE spectral analysis averaged by treatment group.	20
5	Plots displaying the average power spectral density in the delta and theta frequency bands by recording for the treatment group receiving anodal TDCS and demonstrating stimulus artifact.	24
6	Plots displaying the average power spectral density in the alpha and beta frequency bands by recording for the treatment group receiving anodal TDCS and demonstrating stimulus artifact.	25
7	Plots displaying the average power spectral density in the low and high gamma frequency bands by recording for the treatment group receiving anodal TDCS and demonstrating stimulus artifact.	26

8	Multi-taper estimate spectrograms representing the average power spectral density over time of the group of animals receiving anodal TDCS and exhibiting stimulus artifact.	28
9	Multi-taper estimate spectrograms representing the average power spectral density over time of the group of animals receiving anodal TDCS without exhibiting stimulus artifact.	29
10	Plots displaying the average power spectral density in the delta and theta frequency bands by recording for the treatment group receiving cathodal TDCS and demonstrating stimulus artifact.	32
11	Plots displaying the average power spectral density in the alpha and beta frequency bands by recording for the treatment group receiving cathodal TDCS and demonstrating stimulus artifact.	33
12	Plots displaying the average power spectral density in the low and high gamma frequency bands by recording for the treatment group receiving cathodal TDCS and demonstrating stimulus artifact.	34
13	Multi-taper estimate spectrograms representing the average power spectral density over time of the group of animals receiving cathodal TDCS and exhibiting stimulus artifact.	35
14	Multi-taper estimate spectrograms representing the average power spectral density over time of the group of animals receiving cathodal TDCS without exhibiting stimulus artifact.	36
15A	EEG recordings of CoSD events.	39
15B	Spectrograms of EEG recordings of CoSD events.	39
16	Spectrograms demonstrating localization of CoSD event related gamma activation across channels.	41

## LIST OF ABBREVIATIONS

CoSD.....	Cortical spreading depression
EEG.....	Electroencephalogram
IACUC .....	Institutional Animal Use and Care Committee
MCAO.....	Middle cerebral artery occlusion
MTE .....	Multi-taper estimate
MUA .....	Multi-unit activity
NMDA .....	N-methyl-D-aspartate
PBS .....	Phosphate buffered saline
TDCS .....	Transcranial direct current stimulation

## INTRODUCTION

### *Transcranial Direct Current Stimulation*

Transcranial Direct Current Stimulation (TDCS) is a noninvasive neuromodulatory technique in which weak electrical currents are applied through the scalp. An early seminal study by Bindman et al. (1964) in the rat brain showed that applying a positive electrical current to a region of cortex increased the frequency of evoked potential activity, and that applying a negative current decreased evoked potential frequency. In recent years, TDCS has been demonstrated to have a similar effect in humans with anodal stimulation, in which the positively charged anodal electrode is placed on the scalp over the cortical region of interest, producing increased cortical excitability as measured by motor-evoked potential response. Correspondingly, cathodal stimulation, in which the negatively charged cathodal electrode is placed on the scalp, was found to inhibit excitability (Nitsche and Paulus, 2000). These changes in excitability were observed to persist for several minutes beyond the period of stimulation. Nitsche later demonstrated that the short term modulation of excitability due to anodal TDCS was dependent on the activity of sodium and calcium channels (Nitsche et al., 2003). More recent work in mouse motor cortex slices demonstrated NMDA (N-methyl-D-aspartate) receptor and low frequency synaptic activation dependent synaptic potentiation in response to anodal TDCS (Fritsch et al., 2010).

While exact mechanisms underlying the effects of TDCS are still being actively examined and debated (Ruffini et al., 2013), the clinical promise of TDCS in providing a

noninvasive and reversible way of modulating cortical excitability has piqued a great deal of scientific and public interest (Dubljevic et al., 2014). The ability of anodal TDCS to locally modulate cortical excitability has spurred research into its use in treating neurological symptoms characterized by pathologically heightened or inhibited activity in particular regions of the cortex, such as in cases of Parkinson's disease (Broeder et al., 2015), stroke rehabilitation (Stagg and Johansen-Berg, 2013), seizure (Dhamne et al., 2015), and chronic pain (Knotkova et al., 2013).

Although the basic “anodal excitation / cathodal inhibition” model of TDCS is well-demonstrated on a cellular level, particularly in the motor cortex, more recent work has sought to conceptualize correlation between TDCS and behavioral or cognitive effects in a network-dependent manner (Fertonani and Miniussi, 2016). There is correspondingly a small, but increasing, number of studies seeking to use EEG recording to provide a neurophysiological correlate of the cortical effects of TDCS. For example, Accornero et al. (2014) described increases and decreases in human prefrontal area average EEG frequency dependent on the direction of the DC dipole generated. Most similar studies are done in human subjects, use scalp electrodes for EEG recording, and focus on analyzing frequency band power over time. One such study demonstrated that anodal TDCS resulted in an increase in theta, alpha, and beta band power in the periods during and after stimulation, with effects not necessarily being limited to the areas of cortex directly stimulated by electrodes (Mangia et al., 2014). Song et al. (2014) corroborate the observation of an increase in beta band power during the period of anodal stimulation. Another study reported increased delta and theta band activity in the human



prefrontal cortex after anodal TDCS (Miller et al., 2015). A recent neuropsychiatric finding correlated anodal TDCS treatment in the dorsolateral prefrontal cortex with event related synchronization of gamma activity and improved performance on a working memory task among subjects diagnosed with schizophrenia (Hoy et al., 2015).

While there is inconsistent and incomplete evidence on the mechanisms by which TDCS exerts influences on neural activity, cathodal TDCS is thought to produce a widespread reduction in the excitability of stimulated neural tissue, whereas anodal TDCS increases excitability. If such mechanisms of action are accurate, TDCS should be able to control aberrant neurological processes that affect large populations of neurons and contribute to disease. One such phenomenon is cortical spreading depression.

### ***Cortical Spreading Depression***

Cortical spreading depolarization (CoSD), first described by Aristides Leão in 1944, refers to a specific response that has been observed in neurons following exposure to various stresses. The cellular basis of CoSD is the perturbation of the mechanisms maintaining normal ion gradients across neuronal membranes. In healthy neurons, a balance between inward current generated by sodium and calcium channels and outward current generated by sodium pumps and potassium channels produces an isosmotic internal environment with high ion concentration gradients characterized by a membrane potential near -70 mV. In neurons affected by CoSD, pump activity becomes incapable of balancing cation influx resulting intracellular hypo-osmolality, cell swelling, and depolarization of the membrane potential to around -10 mV. Neurons that are thus

depolarized cannot fire action potentials, resulting in localized brain silence. The titular spread of CoSD occurs at around 2-6 mm/min in brain tissue and may be moderated by gap junctions between adjacent neurons (Dreier, 2011). Recent evidence seems to implicate interstitial diffusion of potassium ions as the propagating element of CoSD (Enger et al., 2015). Aiba and Shuttleworth (2012) provide one of the more comprehensive investigations of the neurochemical processes underlying spreading depression. Working with rat hippocampal slices, they identified an initial excitatory period of spreading depression, characterized by presynaptic glutamate release. Activation of NMDA-receptors during this period was correlated with increased duration of depolarization of individual neurons and generally delayed recovery from depression. When neurons were metabolically compromised, their ability to recover from spreading depression was inhibited, resulting in an NMDA-receptor dependent cytotoxicity characterized by the inability to recover from locally elevated levels of  $Ca^{2+}$ .

Broberg et al. (2014) provide perhaps the only comprehensive study on the progression of CoSD via cortically implanted EEG recording. CoSD was initiated via injection trauma or administration of fluorocitrate to the cortex. They describe intracortical “ripple activity”, a characteristic burst of activity in the gamma band frequencies (102-198 Hz or above, peaking at 150-160 Hz), which directly precedes the depression phase of CoSD. During the depression phase, which usually lasted between 4-7 minutes, activity in lower frequency bands was observed to become significantly dampened. Approximately one minute after the beginning of the depression phase, irregular low-frequency spiking was often observed.

One current area of investigation is CoSD as a phenomenon accompanying focal ischemic stroke. CoSD, as detected by a characteristic negative slow potential change and transient depression of electrocorticogram readings, was found to occur frequently in the peri-infarct tissue following human ischemic stroke (Dohmen et al., 2008). CoSD in stroke patients may occur with regular periodicity and appears to enlarge the ischemic lesion with each incidence (Nakamura et al. 2010). Under specific conditions, including high extracellular potassium levels and depletion of NO, CoSD can result in spreading ischemia, in which vasoconstriction of the local neurovasculature propagates along with neuronal depolarization. Spreading depression has been implicated as a contributing factor to the expansion of stroke lesion into the penumbral area (Strong et al. 2007). The management of CoSD, and thus spreading ischemia, therefore holds promise in mitigating the expansion of the infarcted region, and thus brain damage, following ischemic stroke.

### ***Cortical Spreading Depression and Transcranial Direct Current Stimulation***

It is interesting to note that both anodal TDCS and CoSD are correlated with NMDA-receptor activation, as well as  $\text{Ca}^{2+}$  channel activity. It is therefore easy to hypothesize that anodal TDCS might exacerbate CoSD and cathodal TDCS might relieve or prevent it. Indeed, anodal TDCS has been found to accelerate the propagation velocity of CoSD artificially induced by introduction of potassium chloride (KCl) to the cortical tissue of rats (Liebetanz et al., 2006). However the same study failed to produce significant results with cathodal TDCS. Yet in a middle cerebral artery occlusion

(MCAO) model of ischemic lesion in rats, application of cathodal TDCS produced a notable neuroprotective effect, reducing both number of recorded CoSD depolarizations shortly after occlusion and infarct size in treated rats (Notturmo et al., 2014).

## AIMS AND OBJECTIVES

### *Identify the Effects of Anodal and Cathodal TDCS on Baseline Cortical Activity*

Despite the prolificacy of authors on the topic of TDCS, there are few recent major findings utilizing more invasive implanted electrode methods to collect EEG data with greater spatial resolution and, more specifically, the ability to resolve possible variability in the effect of TDCS across cortical laminae. This is most likely because the recent focus on TDCS as a noninvasive clinical procedure makes the invasive implantation of electrodes for recording seem somewhat counter-intuitive, as well as ethically prohibitive in the case of most human experimental subjects. In this study, we have utilized this invasive recording method in an animal model, using an implanted multi-electrode probe to collect EEG recordings from the rat cortex before, during, and after anodal and cathodal TDCS stimulation in a bid to better resolve the effects of such stimulation on frequency band activity both temporally and spatially.

### *Identify the Effect of Anodal and Cathodal TDCS on Cortical Spreading Depression, Using the Occurrence of “CoSD Events” as a Proxy Measure*

Notturmo et al. (2014) provide an excellent jumping off point for the examination of TDCS and its effectiveness in altering CoSD and spreading ischemia. However, the MCAO stroke model is difficult to standardize, often producing irregular regions of ischemia with large penumbra. Instead of complex surgeries, this new project will use injection of potassium chloride into the cortex, similar to the method described in

Liebetanz et al., to directly generate highly focused CSD without ischemia, allowing for the specific study of the CSD phenomenon. Cortical EEG probes will then be used to detect the electrophysiological response to localized CoSD.

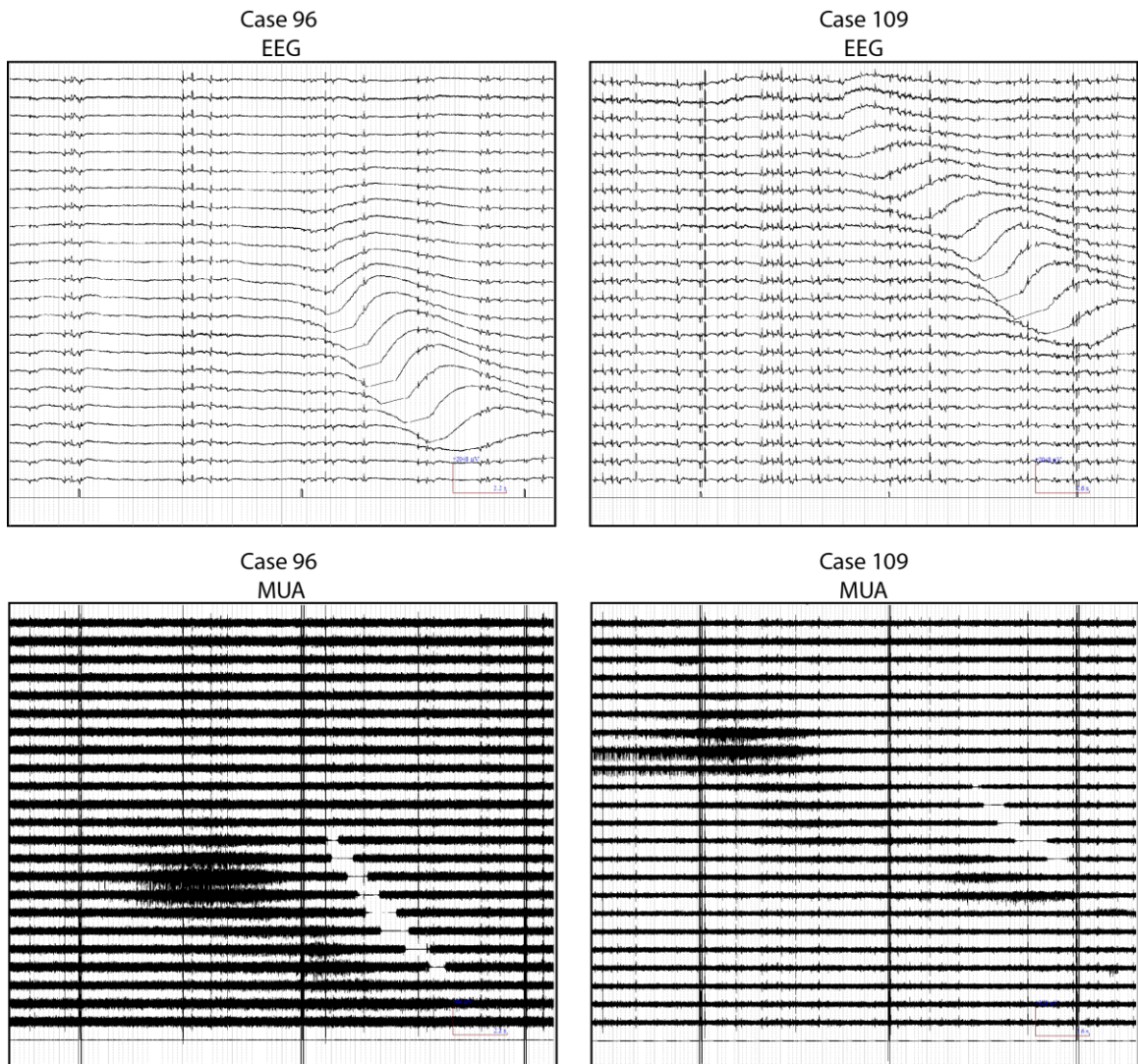


**Figure 1. EEG and multi-unit activity recordings demonstrating characteristics of CoSD events in rats.** These traces were obtained via translaminal recording in the rat cortex after administration of 1  $\mu$ L of KCl to the dura. In these plots, the abscissa represents time and the ordinate axis represents, from top to bottom, 23 recording channels arranged from shallow to deep within the cortex. The EEG and MUA traces for each case have been aligned temporally. The characteristic CoSD event wave pattern can clearly be observed in the EEG traces. Prodromal spiking can be observed in the MUA traces.

Previous work in the Rushmore lab characterized KCl induced CoSD using translaminar multi-electrode recording. One of the unique features of CoSD identified using this method has been what is tentatively called the “CoSD event”. This is a low frequency (in the delta range) bipolar wave defined by a current sink followed by a current source via current source density analysis methods. The wave appears to travel from superficial cortical layers to deeper layers over the period of several seconds, resulting in a striking appearance easily discernible from raw EEG data. Analysis of multi-unit activity (MUA) demonstrated that these events are commonly preceded by a prodromal increase in multi-unit spiking in the channels in which the CoSD event wave begins propagation (Figure 1). It is unclear whether the CoSD events are analogues of the high-frequency ripple activity or the irregular local low-frequency spiking identified by Broberg et al. (2014) or if they are a previously undescribed phenomenon associated with CoSD.

Having identified CoSD events as a reliable correlate of CoSD, we have thought to follow Notturmo et al. (2014) in testing the response of this measure to TDCS treatment in vivo. EEG recordings of the rat cortex will be screened for the presence of CoSD events with and without TDCS treatment.

## METHODS

### *Animals*

Twenty-four (24) male Sprague-Dawley rats at approximately between the ages of 2-3 months were used in this study. Their care and treatment adhered to protocols approved by the Boston University School of Medicine Institutional Animal Care and Use Committee (IACUC). Thirteen (13) animals went on to receive anodal TDCS and eleven (11) went on to receive cathodal TDCS.

### *Surgical Procedure*

Rats were first weighed, then injected with 160 mg/kg of intraperitoneal chloral hydrate for initial sedation. Glycopyrrolate was concurrently administered intraperitoneally at 0.02 mg/kg to reduce bronchial secretions and improve breathing under anesthesia. Following 5 minutes, 50 mg/kg of intraperitoneal pentobarbital was administered to induce anesthesia. Level of pain response was measured periodically during surgery via tail pinch reflex, and intraperitoneal pentobarbital was administered as needed throughout the procedure to maintain full suppression of pain response.

Once full anesthesia had been achieved, rats were placed into a stereotactic apparatus and secured with ear bars positioned into the ear canals of the animals such that lateral movement of the skull was largely constrained. Dorso-ventral movement of the skull was further constrained by gently pinching the snout of the rats in an incisor bar, immobilizing the head. Ophthalmic ointment was daubed onto the corneal surface in



order to reduce irritation. A lubricated temperature probe was inserted rectally and secured with surgical tape to the tail. The probe was connected to a temperature monitor providing feedback to a heating pad placed underneath the animal torso, allowing the core temperature of the animal to be kept at around 37.7°C.

An initial scalpel incision was made at the midline of the skull. Skin and fascia were retracted and clamped with hemostats to reveal the surface of the skull. A bone scraper was used to remove excess tissue on the skull surface to reveal skull sutures. The skull surface was cleaned with saline and the stereotactic coordinates for lambda were measured. Sites for drilling burr holes were measured and labeled with a marker. Three drill sites were marked relative to lambda for each animal at 0.5mm anterior and 3.5mm to the right, 0.5mm anterior and 3.5mm to the left, and 10mm anterior and 2.3mm to the left. Burr holes were made at these sites with an electric drill, revealing the surface of the dura mater. Two additional shallower holes, not deep enough to penetrate entirely through the skull, were drilled approximately 2.5mm to the right and 1mm anterior and posterior of bregma. One ground electrode was screwed into each of the two shallower holes and both were connected to a preamplifier. A recording probe was then attached to the preamplifier and sunk into the burr hole drilled 0.5mm anterior and 3.5mm to the left of lambda to a depth of approximately 3mm from the surface of the dura based on visual inspection of electrode penetration. A concentric bipolar stimulating electrode was sunk into the burr hole drilled 0.5mm anterior and 3.5mm to the right of lambda to a depth of 2mm.

### ***Electroencephalogram (EEG) Recording and Paired Pulse Stimulation Setup***

EEG recordings were captured with a Plexon U-probe, containing 23 linearly arranged platinum-iridium electrodes spaced 50 microns apart. The probe was sunk into the rat brain such that the recording electrodes were arranged vertically within the motor cortex from shallow to deep. The recording electrode was connected to a preamplifier affixed to a stereotactic arm with a Preci-dip pin connector. The preamplifier was then connected to a main amplifier (Neurotrack Systems) linked to a computer running LabView software (National Instruments) allowing for monitoring and controlling of EEG recording. The preamplifier was grounded by two electrodes screwed into the skull. Data was collected at a sampling rate of 4000 Hz. Hardware filters separated collected data into high (100-5000 Hz) and low (0.2-500 Hz) frequency bands, which were saved respectively as EEG and multi-unit activity (MUA) data files.

A bipolar stimulating electrode was used to generate two 800mA bipolar electric pulses spaced by 100usec contralateral to the recording probe every 10 seconds. The stimulation amplitude was controlled by two serially linked Iso-Flex stimulus isolators (AMPI Instruments) which were connected to a Master-8 stimulator dictating stimulation periodicity and duration. Paired pulse and MUA data were collected but not analyzed for this study.

### ***TDCS Setup***

An ActivaDoseII (Patterson Medical) iontophoresis device was used to power TDCS. The device was connected via alligator clips to self-adhering Uni-Tab stimulating

electrodes (Covidien) custom trimmed into 0.5x1.5 cm<sup>2</sup> rectangles with rounded corners. For anodal TDCS, the positive electrode was adhered to the area of the exposed skull approximately half a centimeter anterior to the recording electrode, to the left of the sagittal suture. The negative return electrode was placed on the denuded skin of the back between the shoulder blades. Return electrode conductivity and adherence was improved by daubing with Elefix conductive EEG paste (Nihon Kohden) prior to placement. For cathodal TDCS, the placement of the electrodes was reversed; the negative electrode was placed on the skull and the positive electrode was placed on the back. In both anodal and cathodal cases, TDCS was conducted at 0.1mA for 5 minutes.

#### ***Potassium Chloride (KCl) Drop Setup***

Ten microliters of 3M KCl were drawn into a 10uL Neuros injection syringe (Hamilton). The syringe was attached to a manipulable arm and placed such that the tip of the syringe was stably positioned at the burr hole drilled at 10mm anterior and 2.3mm to the left of lambda, a few millimeters above the dura. Cortical spreading depression was initiated by administering KCl solution via syringe to the surface of the dura.

#### ***Experimental Procedure and Data Collection***

Once recording, paired pulse stimulation, and TDCS electrodes were placed, the animal was given an appropriate dose of pentobarbital based on level of pain response and left to rest for 30 minutes. Recording was subsequently initiated. Each animal

experienced four consecutive recording blocks consisting of five 5-minute recordings each.

Block 1, Baselines: EEG baselines were recorded. Five consecutive baseline recordings of 5 minutes each were collected.

Block 2, TDCS only: TDCS was administered for 5 minutes concurrently with EEG recording. Four consecutive 5 minute recordings were collected directly after TDCS.

Block 3, KCl only: 1uL of KCl was administered from the previously positioned syringe to the surface of the dura, coinciding with the beginning of a 5 minute recording period, followed by four subsequent 5 minute recordings.

Block 4, TDCS and KCl together: TDCS and a 5 minute recording period were initiated simultaneously with the drop of another 1uL dose of KCl. The four subsequent 5 minute recordings in this block bring the total number of recordings per animal up to 20.

Intraperitoneal pentobarbital was given to animals in between recording periods in 0.1mL doses as needed. In general, pentobarbital was administered in the middle of a recording block rather than at the beginning in order to avoid conflation of treatment effects with the effect of anesthesia.

### ***Perfusion Procedure***

After the conclusion of data collection, the animal was given a lethal dose of intraperitoneal pentobarbital (>150mg/kg). Although the main source of data in this study was electrophysiological, animal brains were preserved and collected in order to retain

physical evidence of appropriate recording probe and stimulating electrode placement. The animal was removed from all apparatus and moved to a designated location for perfusion. During perfusion, the animal's chest was opened and the heart was injected with 0.05mL of heparin at 1000 units/mL and 0.05mL of 1% sodium nitrite. A cannula was inserted into the aorta via the left ventricle and clamped in place at the ventricle with a hemostat. A solution of 3.7% formalin in 0.1M PBS was continually perfused into animal through the cannula to a total volume of 450mL. The animal's head was then removed and the brain removed from the cranial vault with rongeurs. The brain was placed into perfusion solution and stored in the refrigerator at 4°C.

After one or more days, brains were transferred from perfusion solution into 10% glycerol with 2% DMSO and further transferred after one or more days into 20% glycerol with 2% DMSO. Brains could then be cut into slices via microtome for histological analysis or frozen for storage at -80°C.

### ***Analyzing the Effect of TDCS on Baseline Activity***

EEG data from the first two blocks of recording were analyzed in order to determine the effect of anodal and cathodal stimulation on baseline cortical activity. Raw EEG data were processed using Matlab (Mathworks) and its associated signal processing toolbox. EEG recordings were first divided into discrete 10-second blocks, from which 9-second epochs were extracted for wavelength analysis. Each epoch was subjected to fast Fourier transform analysis with hamming windowing using the Matlab "periodogram" function. The generated frequency spectra were then averaged across all epochs for each

recording. The average frequency spectrum data for each recording was further separated into frequency bands: delta (1-4 Hz), theta (4-9 Hz), alpha (9-14 Hz), beta (14-31 Hz), low gamma (31-81 Hz), and high gamma (81-151 Hz). The power within each designated band was then averaged, producing discrete values representing the average power across a given EEG recording within individual frequency bands. These average frequency band power data were normalized to account for variation in baseline activity by dividing all values across channels and recordings for a given animal by a normalization constant calculated by averaging the sum of the average power across the six frequency bands across channels for each recording and further averaging the resultant values from the five baseline recordings. The final datasets were obtained by splitting the animals into groups and averaging the normalized average frequency band power data by group. Animals were segregated into one of four treatment groups based on whether they were subjected to anodal or cathodal TDCS and whether or not a transient increase in alpha and/or beta band activity was observable during the period of TDCS treatment. The presence of this transient alpha/beta activity, or “stimulus artifact” was chosen as a proxy for response to TDCS.

To observe the finer details of changes in frequency spectra over time, multi-taper estimate (MTE) spectral analysis using the Chronux toolbox for Matlab was applied to generate moving window spectrogram data for individual recordings. Recordings were first trimmed to matching lengths across animals by treatment group. The recordings capturing the period of TDCS stimulation were specially trimmed such that periods of stimulation across animals were aligned. MTE spectral analysis was then run on the

trimmed data using the Chronux “mtspecgramc” function with a moving window size of 3 seconds, a step size of 0.3 seconds, a time-bandwidth product of 4, and 7 tapers (Bokil et al., 2010). Spectrogram data were normalized using a normalization constant calculated for each animal by averaging the sum of power across frequencies across time points and channels for each recording and further averaging the resultant values from the five baseline recordings. Finally, normalized spectrogram data were averaged by treatment group.

Data was not averaged across recording channels, allowing for comparison of data from the 23 separate recording electrodes on the EEG probe, arranged from shallow to deep within the rat cortex.

### ***Observing the Effect of TDCS on Cortical Spreading Depression Events***

EEG data from the second two recording blocks, during which KCl was administered to induce CoSD, were parsed in order to determine the effect anodal or cathodal TDCS might have on the occurrence of CoSD events.

The first recording in the third recording block, the recording during which animals experienced only KCl administration, was screened for each animal. Animals that did not exhibit a CoSD event in the first 5 minutes after administration of KCl during the third recording block were removed from further analysis. The first recording in the fourth recording block, during which animals experienced simultaneous KCl administration and TDCS treatment, was subsequently screened for CoSD events. CoSD events were screened for by visual examination of raw EEG data.

## RESULTS

### *Experimental Setup and Data Processing*

Figure 2 shows a schematic of the experimental setup. A multi-contact recording electrode was placed in the cerebral cortex of the rat brain and connected to an amplifier (triangle). The recording electrode consisted of 23 evenly spaced contacts (inset, middle), which recorded individual EEG traces (right) simultaneously from all 23 channels, from shallow to deep within the cortex.

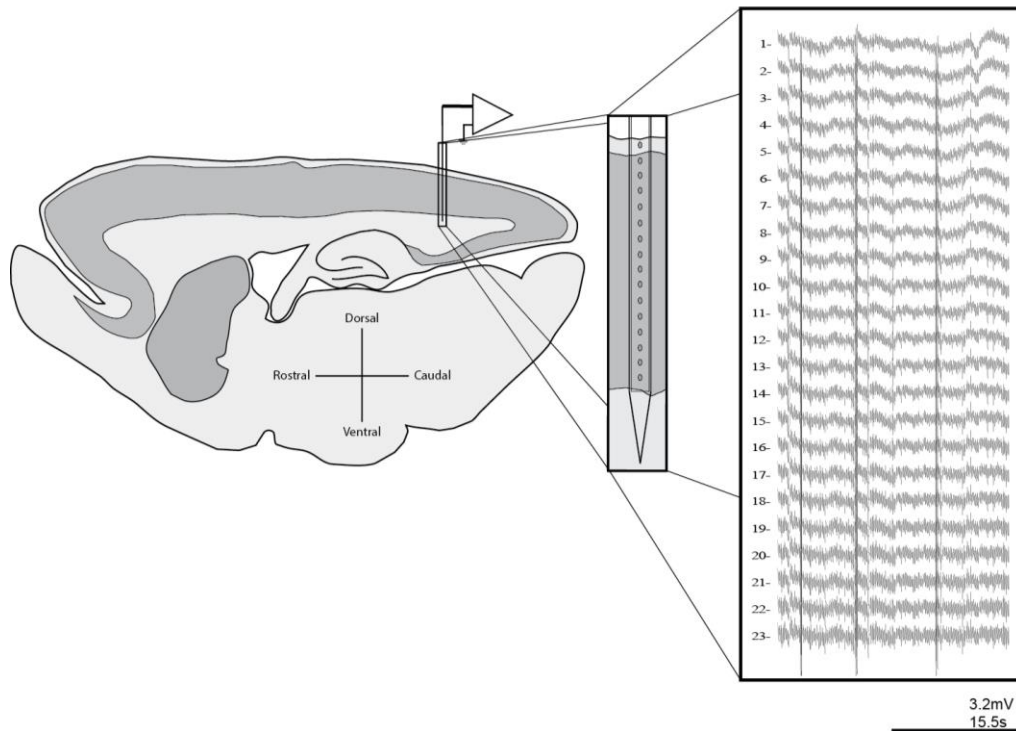


**Figure 2. Schematic of parasagittal section of the rat brain demonstrating the approximate recording electrode placement.** Dark grey shading represents grey matter, and light grey shading represents white matter. The middle inset displays the position of the electrode contacts relative to the grey matter and the right inset shows an example of 23 channel EEG data derived from cortical recording.



The raw EEG data were processed via power spectral density analysis using the Matlab “periodogram” function, then averaged over epochs by recording to produce one power spectrum representative of each recording. Figure 3A demonstrates an example of raw periodogram data averaged over epochs for a single recording. The periodogram was then separated based on frequency bands, as indicated by colors. The mean power for each frequency band was plotted across the recording session for each individual channel.

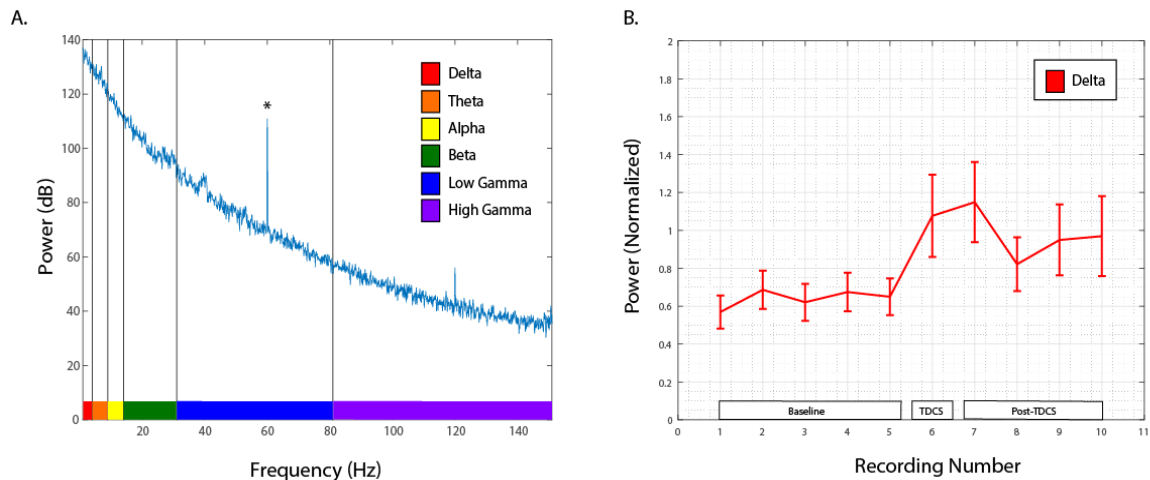


**Figure 3A. Power spectral density representation of a single recording.** Data are the result of averaging over many epochs extracted from the raw EEG data. The colored bands at the bottom of the plot delineate the six frequency bands that were analyzed.

**Figure 3B. Plot displaying change in average normalized power over multiple recordings for a particular frequency band and treatment group for a single channel.** Recording blocks 1 and 2 are represented. Error bars represent error from averaging over treatment group members.

The data were then normalized to baseline for each animal and averaged for each EEG frequency band. This approach produced data representing the average EEG power within designated frequency bands for each channel. Standard error of the mean was calculated for the mean data from multiple animals by treatment group. Figure 3B displays an example of the final result of data processing, a plot demonstrating changes in power over time for a given frequency band and treatment group for a single channel.

The EEG data were also processed into spectrograms, using multi-taper estimated (MTE) spectral analysis software to visualize power spectral density in the delta, theta, alpha and beta bands over time. Figure 4 shows an example of a spectrogram from one channel in which the color illustrates the power, the ordinate represents the frequency, and the abscissa represents time. Notice that at a certain point in the middle of the experiment, immediately after the initiation of anodal TDCS, the power at frequencies between 1 and 4 Hz increased in power. Also notice the diverging shape at around 12 Hz.

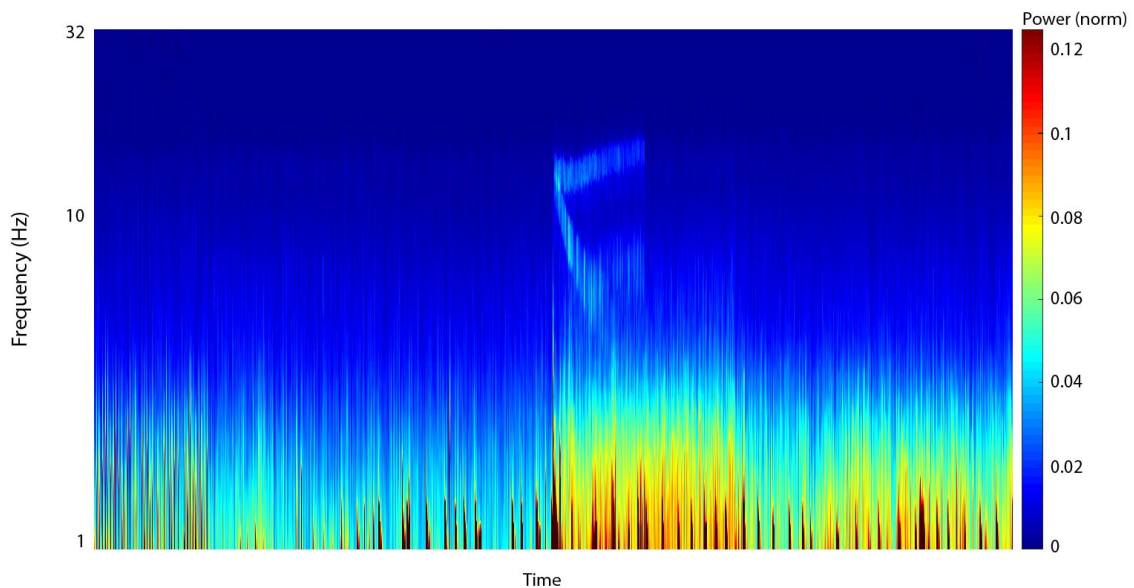


**Figure 4. Plot of spectrogram data from MTE spectral analysis averaged by treatment group.** The time axis of this plot represents the linear concatenation of the ten recordings from recording blocks 1 and 2. This type of plot allows for the observation of fine changes in spectral density over time.

The experimental setup was such that a hole was created in the skull rostrally to the recording electrode for the introduction of KCl in order to initiate cortical spreading depression (CoSD). A TDCS electrode was placed on the skull surface between the burr

hole and the recording electrode. During the experimental procedure, animals experienced four blocks of recording: baselines, TDCS only, CoSD only, and TDCS with CoSD. The first two blocks were analyzed to determine changes in power spectral density before, after, and during TDCS treatment. The second two blocks allowed for assessment of the effect of TDCS on cortical spreading depression.

The following sections divide the results into two categories. In the first section, the effect of TDCS on baseline cortical activity is discussed. In the second section, the effect of TDCS on cortical spreading depression is considered.

### ***The Effect of TDCS on Baseline Cortical Activity***

#### *Segregation of Groups*

During the data collection process, some animals exhibited a clear increase in alpha and/or beta band activity corresponding with the exact duration of active stimulation, while the remainder exhibited no trace of such activity. Whether due to experimental or subject factors, response to treatment with TDCS is highly variable, as demonstrated in numerous studies in humans (Horvath et al., 2014; López-Alonso et al., 2014). In this study, the binary presence or absence of a spike in alpha/beta band activity concurrent with stimulation during the second recording block allowed for experimental groups to be cleanly divided based on TDCS response. This activity spike was considered to be an artifact of the stimulation, since increasing the magnitude of stimulation increased the amplitude of the signal. Within anodal and cathodal TDCS treatment groups, animals exhibiting stimulus artifact were considered TDCS responders and those that did not were

considered TDCS non-responders. The sizes of each treatment group were proportioned as follows: anodal with stimulus artifact,  $n = 8$ ; anodal without stimulus artifact,  $n = 5$ ; cathodal with stimulus artifact,  $n = 4$ ; cathodal without stimulus artifact,  $n = 6$ . One animal was excluded from further analysis after preliminary examination due to particularly erratic EEG response during baseline recordings.

For analysis, the first two blocks of recordings for each animal were combined to yield 10 recordings per animal in three groupings: baseline (recordings 1-5), TDCS (recording 6), Post-TDCS (recordings 7-10). In the following figures (Figures 5-7 and 10-12), the average power across these recordings is illustrated for each of the 23 recording channels according to frequency band. For each subgraph, recording segment number is on the abscissa, and the ordinate reflects normalized mean power. Thus, the data for channel 1 is in the upper left of each figure, and the channel number increases from left to right and subsequently from top to bottom.

#### *Group 1: Anodal TDCS with Stimulus Artifact*

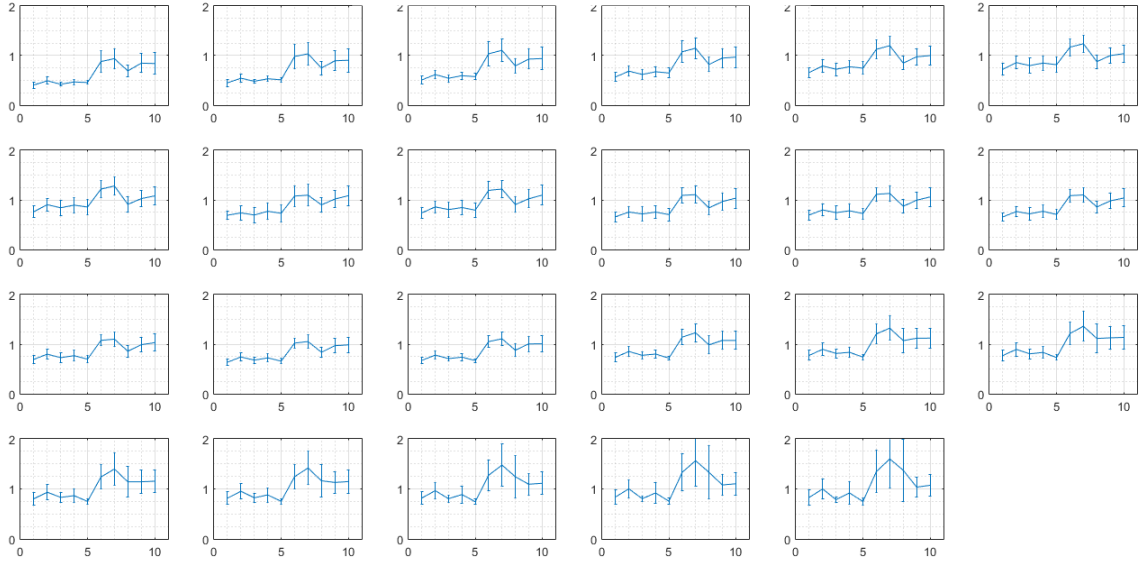
In the anodal with stimulus artifact (SA) group, delta band power increased across channels during TDCS stimulation and remained elevated for one 5 minute recording period post-TDCS (Figure 5).

Similarly, theta band power exhibited a sharp increase in power across channels during TDCS, with a partial decline during the first post TDCS recording, and a return to baseline at the second (Figure 5).

The alpha and beta bands exhibited highly variable spikes in activity during the TDCS treatment period only. This increase in activity corresponds to the presence of the previous discussed stimulus artifact (Figure 6).

Increase in power of low gamma and high gamma activity in the period after TDCS may be correlated to stimulation, but this increase in power over time is much less clear relative to activity in lower frequencies and may be an artifact of consistency in anesthetic regime across animals. Elevated high gamma band power in the last two recordings post-TDCS exhibits correspondingly high standard error. This elevation corresponds to the apparent increase in power in the last two recordings in the delta and theta bands relative to baseline. Very strong low gamma activity in the second channel across recordings appears to be due to 60 Hz electrical noise (Figure 7).

Anodal TDCS with Stimulus  
Artifact: Delta



Anodal TDCS with Stimulus  
Artifact: Theta

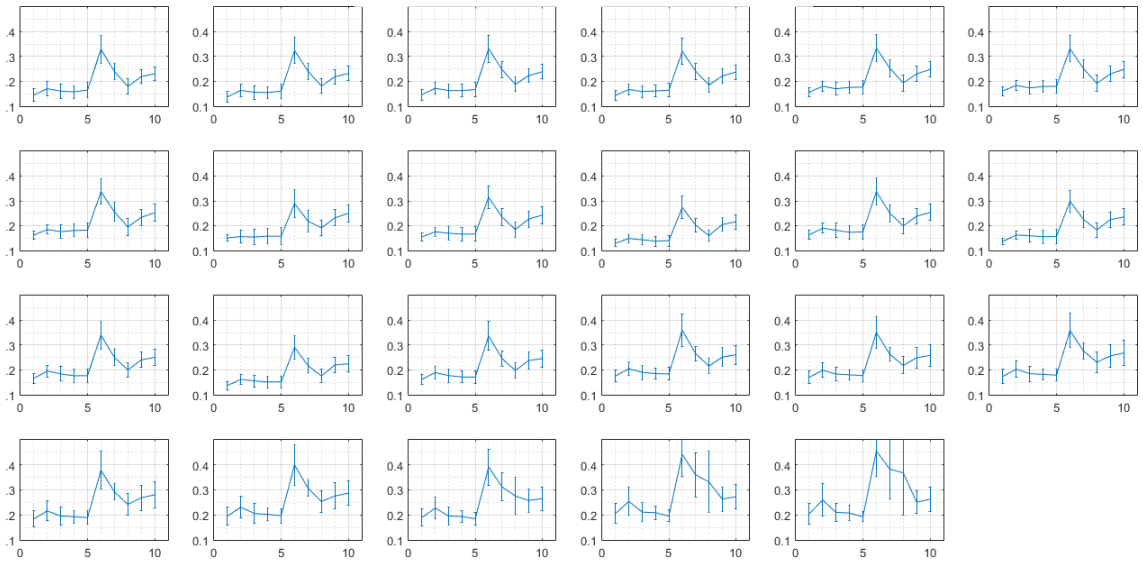
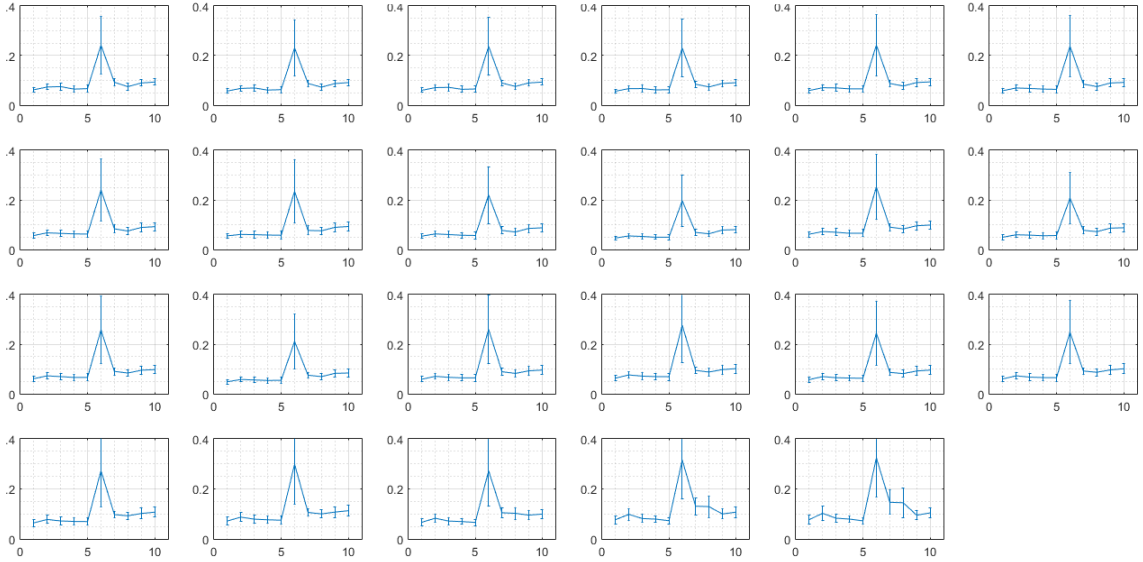


**Figure 5. Plots displaying the average power spectral density in the delta and theta frequency bands by recording for the treatment group receiving anodal TDCS and demonstrating stimulus artifact.** TDCS was administered throughout the 6<sup>th</sup> recording. Each subplot represents one of the separate 23 recording channels, arranged by increasing channel number from left to right and from top to bottom. For each subplot, the abscissa represents recording number and the ordinate represents normalized mean power.

Anodal TDCS with Stimulus  
Artifact: Alpha



Anodal TDCS with Stimulus  
Artifact: Beta

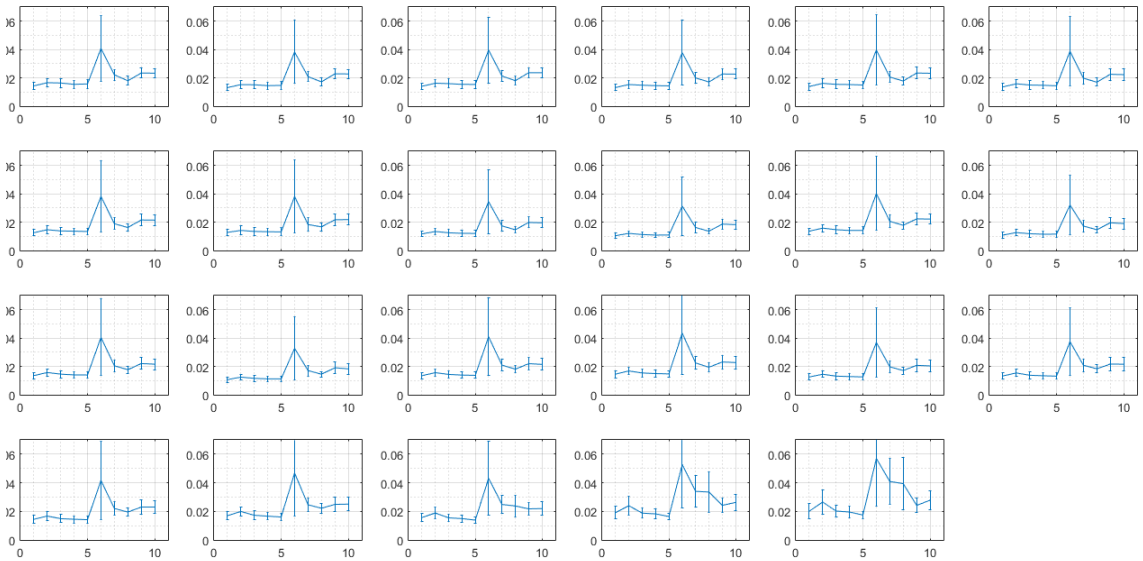
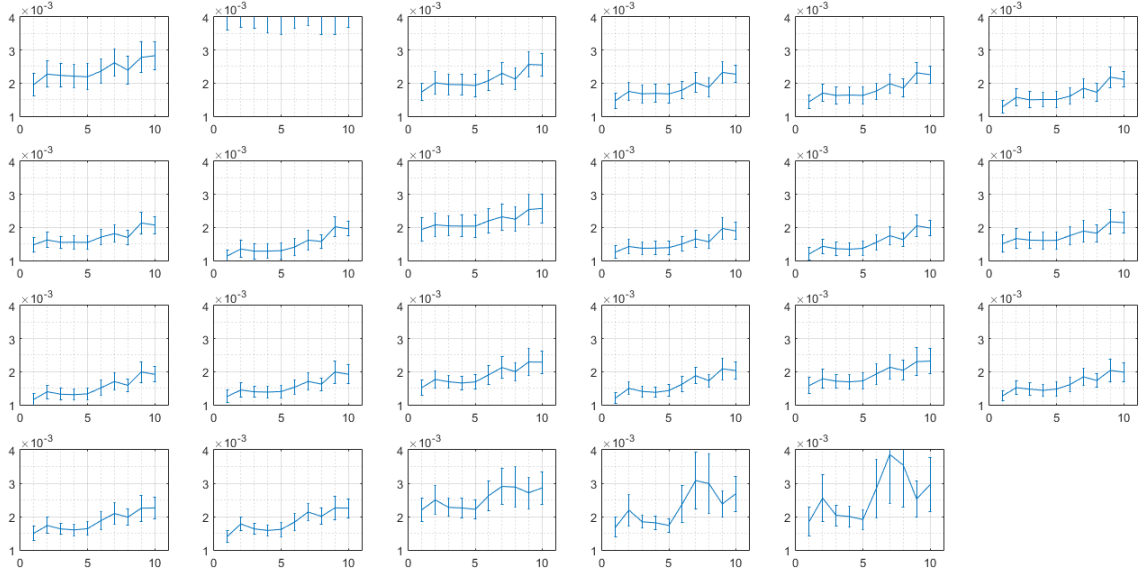


**Figure 6. Plots displaying the average power spectral density in the alpha and beta frequency bands by recording for the treatment group receiving anodal TDCS and demonstrating stimulus artifact. TDCS was administered throughout the 6<sup>th</sup> recording. Subplots are as described in Figure 5.**

Anodal TDCS with Stimulus  
Artifact: Low Gamma



Anodal TDCS with Stimulus  
Artifact: High Gamma

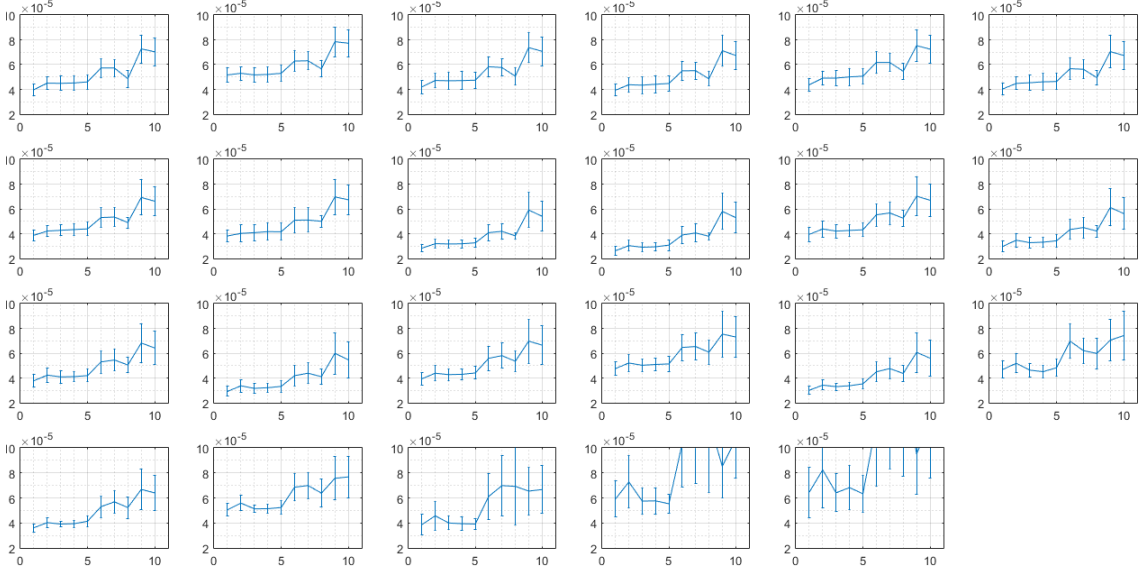


**Figure 7. Plots displaying the average power spectral density in the low and high gamma frequency bands by recording for the treatment group receiving anodal TDCS and demonstrating stimulus artifact. TDCS was administered throughout the 6<sup>th</sup> recording. Subplots are as described in Figure 5.**



The effects of TDCS appear to be consistent in all frequency bands across channels, aside from exaggerated increases in power and greater standard error for measurements in the lower channels. However, the primary contributor to these effects appears to be one outlier animal which seemingly exhibited idiosyncratically high EEG activity in the deep cortex.

The spectrogram representation of the data corroborates the frequency band analysis by demonstrating a marked increase in delta and theta frequency activity directly after the initiation of TDCS and lasting throughout the period of stimulation and for approximately five minutes afterwards. The spike in alpha and beta activity throughout the stimulation period is also clearly visible (Figure 8).

#### *Group 2: Anodal TDCS without Stimulus Artifact*

In the anodal without SA group, power in the delta, theta, alpha, and beta frequency bands appear mostly constant with a slight increase over time across all recordings with little variation across channels.

Activity in the low gamma band is similarly uneventful, but much more variable. Very strong low gamma activity in the second channel across recordings again appears to be due to ambient 60Hz noise. High gamma activity is similarly variable, especially in more shallow channels, with deeper channels exhibiting less variability and the lowest channels showing a possible increase power after TDCS treatment.

The spectrogram representation of the data corroborates the slow increase in power in the delta and theta bands over time (Figure 9).

### Anodal TDCS with Stimulus Artifact

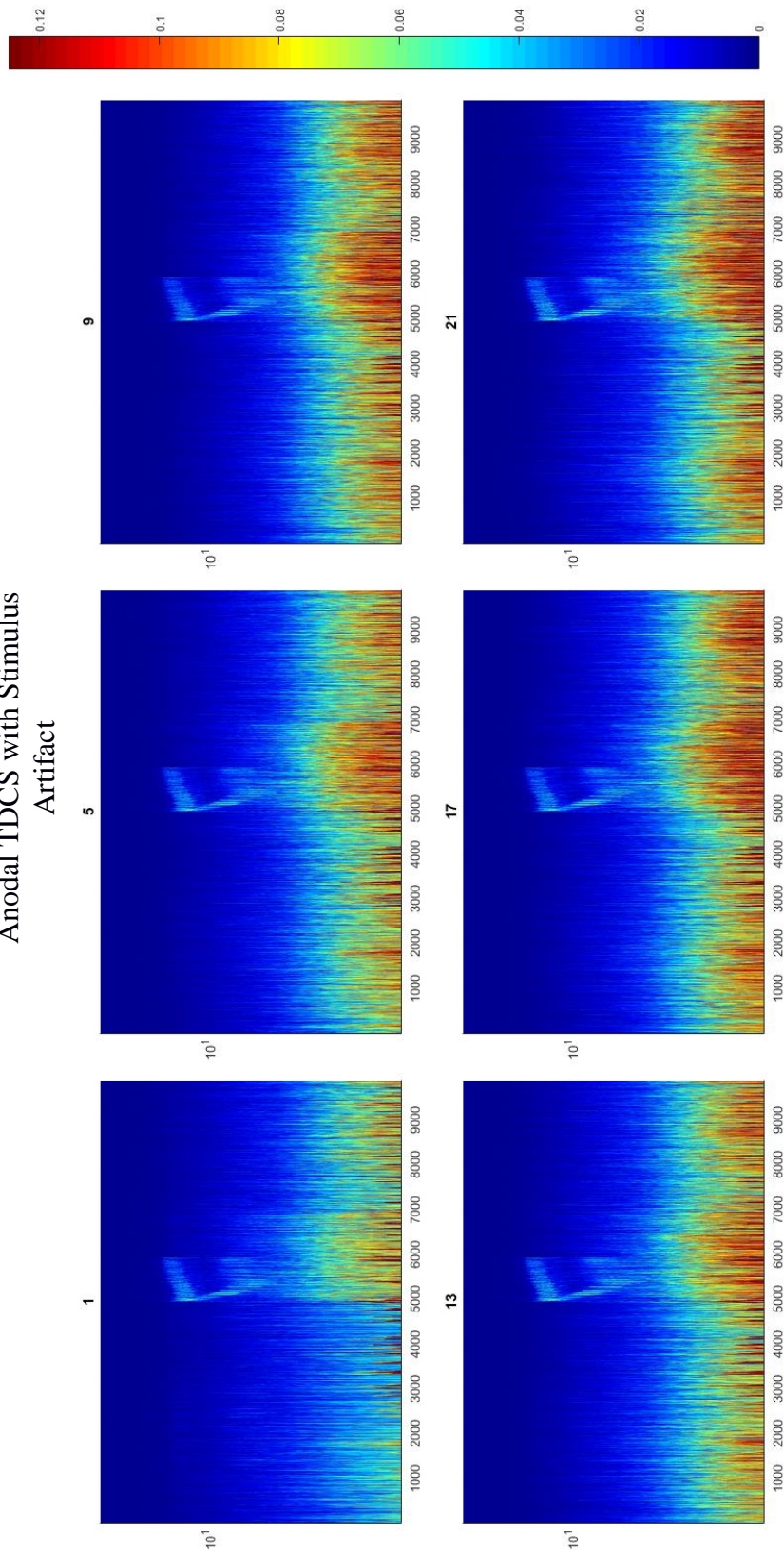


**Figure 8. Multi-taper estimate spectrograms representing the average power spectral density over time of the group of animals receiving anodal TDCS and exhibiting stimulus artifact.** For each spectrogram the abscissa denotes time in number of moving window steps and the ordinate axis denotes frequency from 1-32 Hz on a logarithmic scale. Each moving window step corresponds to 0.3 seconds of actual recording time. Each spectrogram represents data from ten recordings concatenated in time. Color indicates normalized mean power, and the number above each graph reflects the channel, where smaller numbers are more superficial and larger numbers are from deeper electrodes. A sample of electrodes were extracted for clarity.

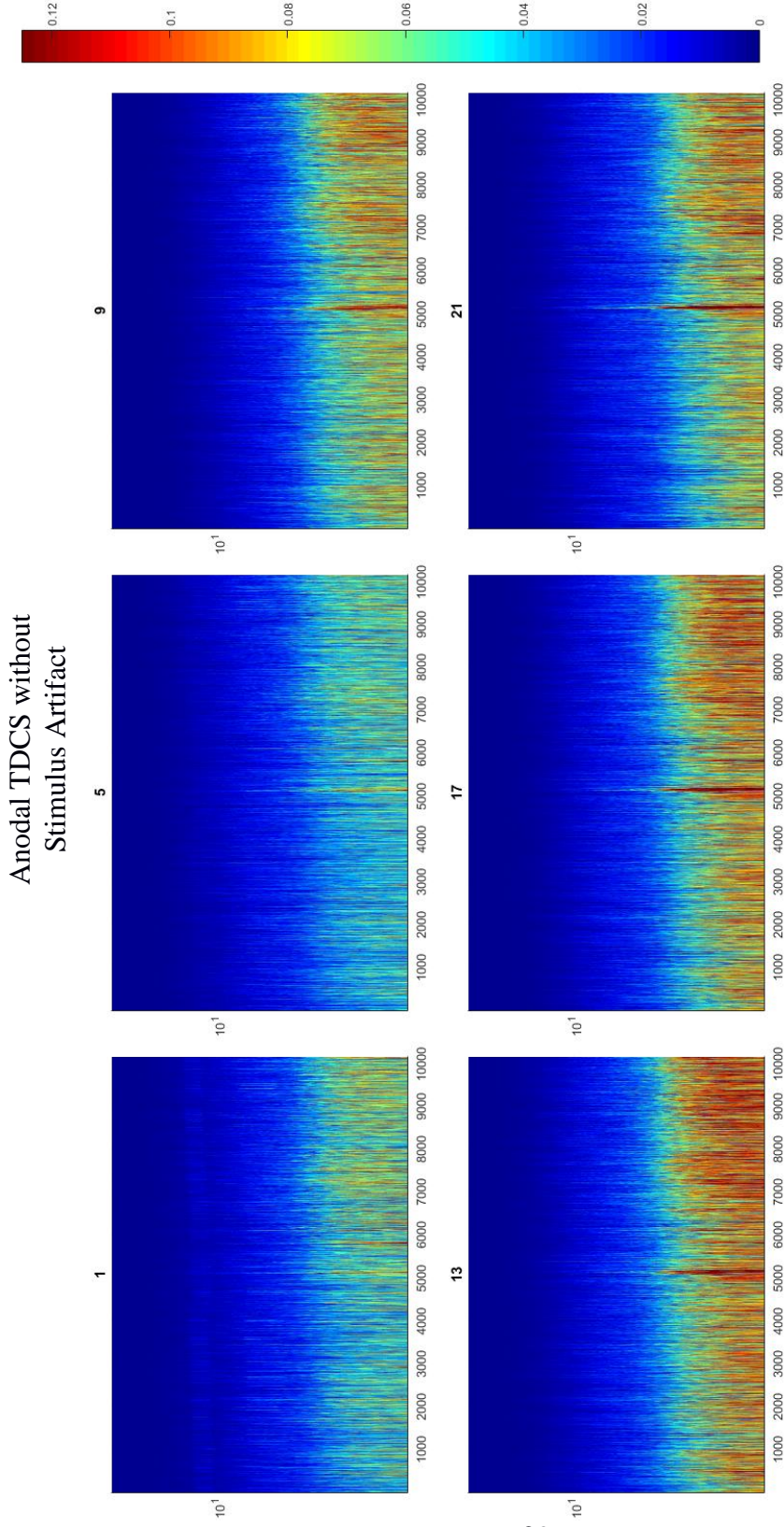


**Figure 9. Multi-taper estimate spectrograms representing the average power spectral density over time of the group of animals receiving anodal TDCS without exhibiting stimulus artifact.** For each spectrogram the abscissa denotes time in number of moving window steps and the ordinate axis denotes frequency from 1-32 Hz on a logarithmic scale. Each moving window step corresponds to 0.3 seconds of actual recording time. Each spectrogram represents data from ten recordings concatenated in time. Color indicates normalized mean power.

### *Group 3: Cathodal TDCS with Stimulus Artifact*

In the cathodal with SA group a slight increase in theta activity following stimulation was observed. The high level of activity during the first two baseline recordings in the delta frequencies in channels 13 and deeper prior to TDCS is noticeable in both the frequency band plots and spectrograms, but the high standard error for these measurements as apparent from the frequency band data suggests the presence of an outlier (Figure 10).

Beta and alpha activity are very constant over time exhibiting only a slight increase in activity during the stimulation period. This corresponds with the observation that the stimulus artifact is smaller during cathodal stimulation compared to anodal given the same stimulation strength (Figure 11).

Activity in low and high gamma bands appears very variable, though mostly constant. However, both, especially high gamma, exhibit possible increases in power during stimulation (Figure 12).

The spectrogram representation of the data corroborates the lack of clear response to TDCS in the delta and theta frequencies, the general dip in activity in the two baseline recordings directly prior to stimulation, as well as the presence of an alpha/beta frequency stimulus artifact which is comparatively quite weak relative that observed during anodal stimulation (Figure 13).

*Group 4: Cathodal TDCS without Stimulus Artifact*

In the cathodal without SA group, a similar degree of apparent increase in theta and delta band both during the baseline recordings and after TDCS stimulation make it difficult to attribute the post-TDCS increase in activity to the effect of TDCS.

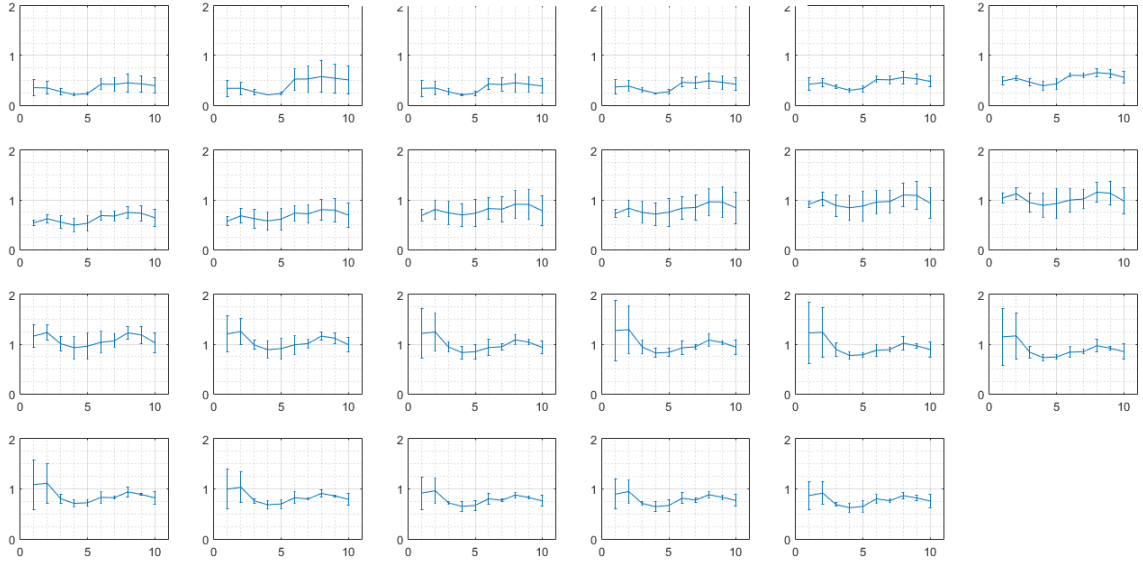
Additionally, neither apparent increase is particularly significant relative to standard error.

Beta and alpha activity in this group appear constant over time with low variability. Low gamma and high gamma activity appear uneventful, exhibiting similar slight elevations in activity in both the pre and post-TDCS periods in the lower channels with moderate variability.

The spectrogram representation of the data corroborates the general lack of response to stimulation (Figure 14).

### Cathodal TDCS with Stimulus

#### Artifact: Delta



### Cathodal TDCS with Stimulus

#### Artifact: Theta

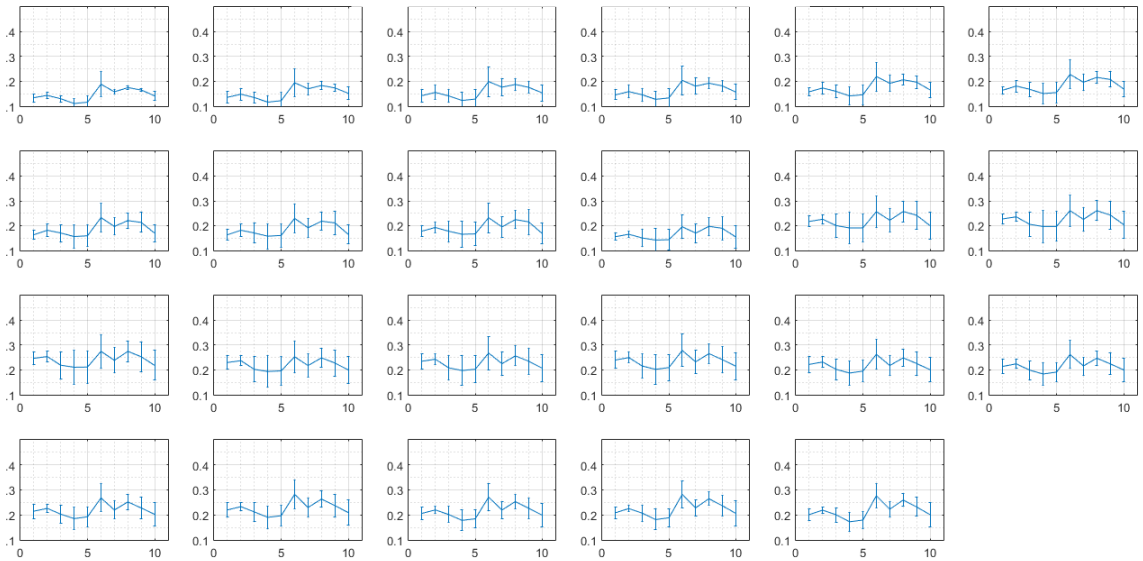
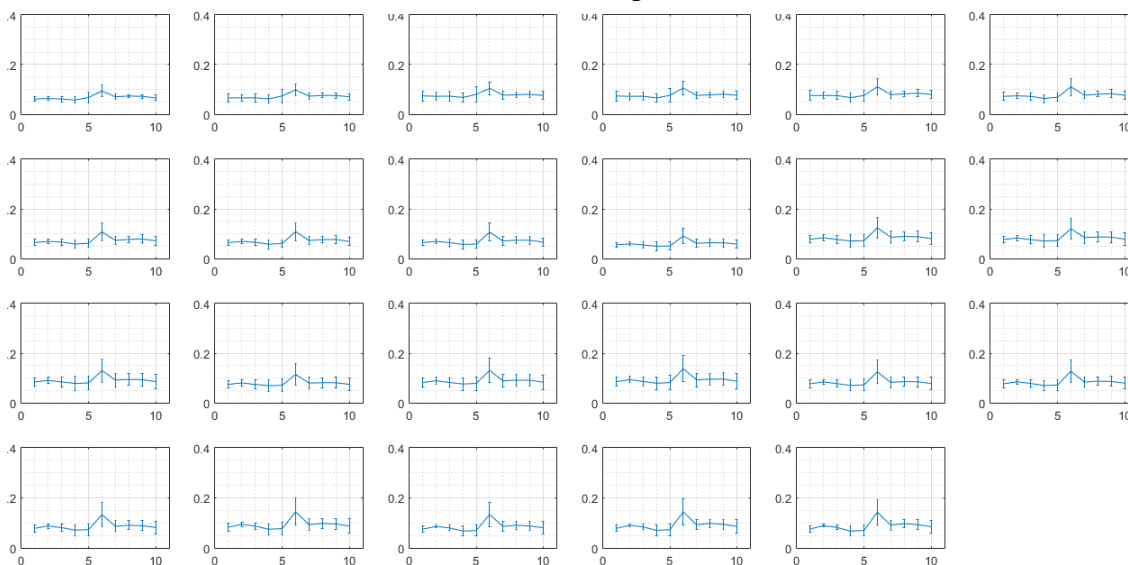


**Figure 10.** Plots displaying the average power spectral density in the delta and theta frequency bands by recording for the treatment group receiving cathodal TDCS and demonstrating stimulus artifact. TDCS was administered throughout the 6<sup>th</sup> recording. Subplots are as described in Figure 5.



Cathodal TDCS with Stimulus  
Artifact: Alpha



Cathodal TDCS with Stimulus  
Artifact: Beta

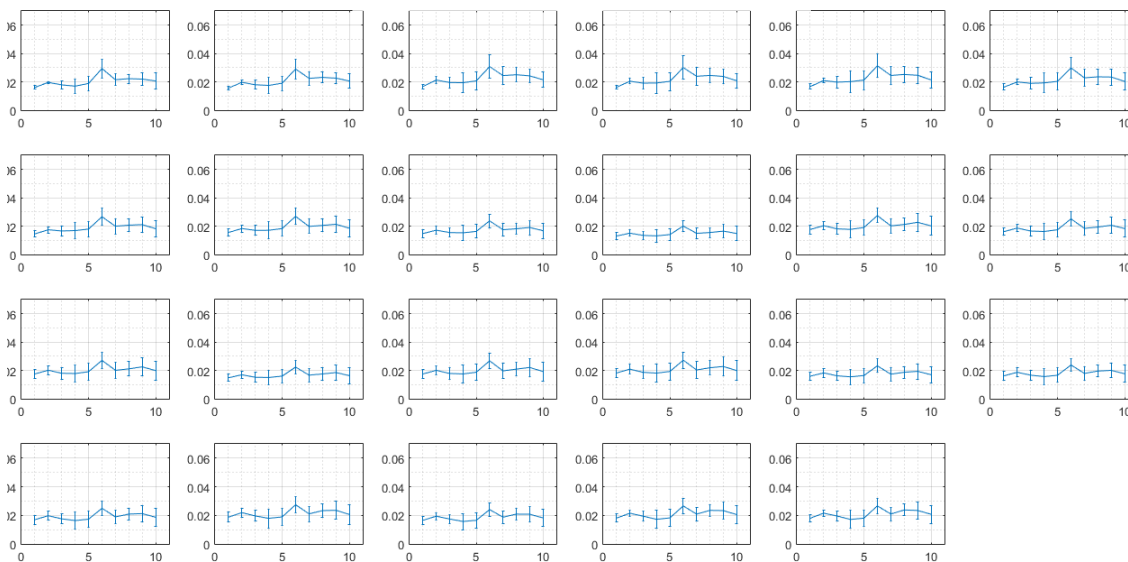
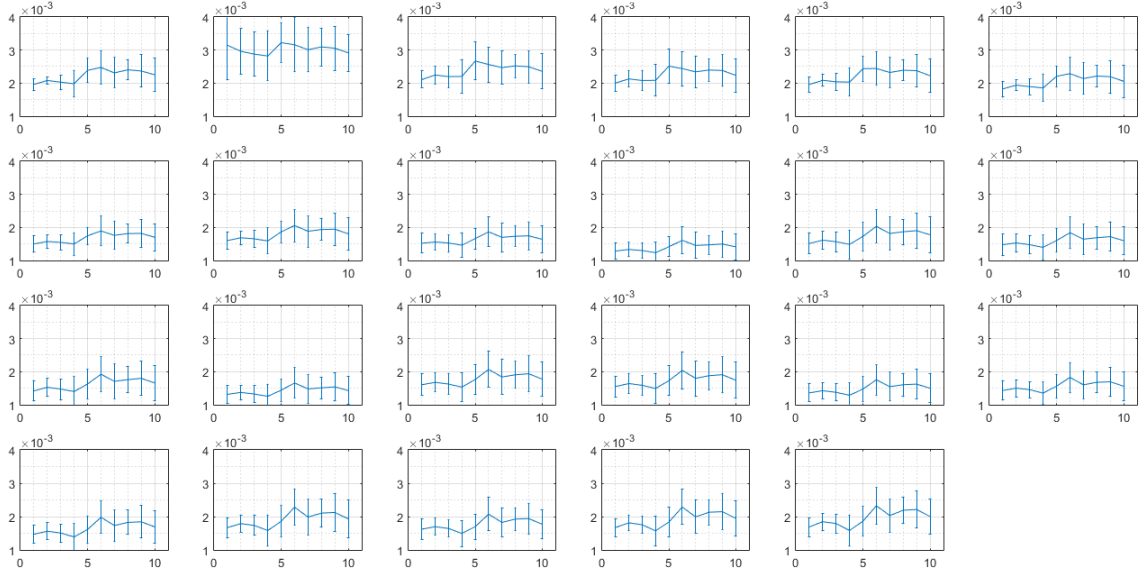


**Figure 11. Plots displaying the average power spectral density in the alpha and beta frequency bands by recording for the treatment group receiving cathodal TDCS and demonstrating stimulus artifact. TDCS was administered throughout the 6<sup>th</sup> recording. Subplots are as described in Figure 5.**

Cathodal TDCS with Stimulus  
Artifact: Low Gamma



Cathodal TDCS with Stimulus  
Artifact: High Gamma

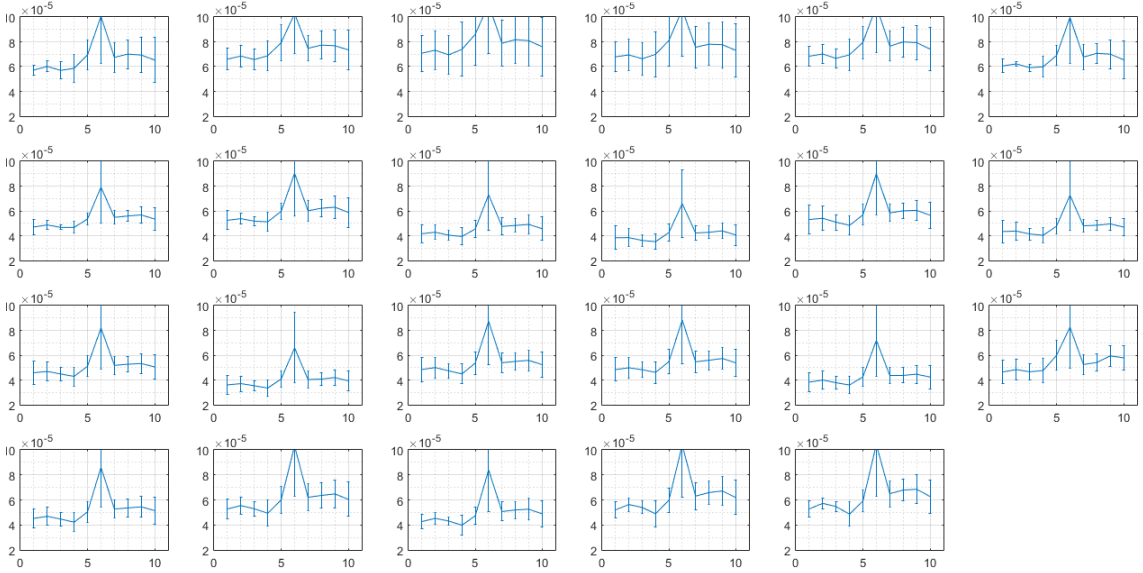


**Figure 12. Plots displaying the average power spectral density in the low and high gamma frequency bands by recording for the treatment group receiving cathodal TDCS and demonstrating stimulus artifact. TDCS was administered throughout the 6<sup>th</sup> recording. Subplots are as described in Figure 5.**



### Cathodal TDCS with Stimulus Artifact

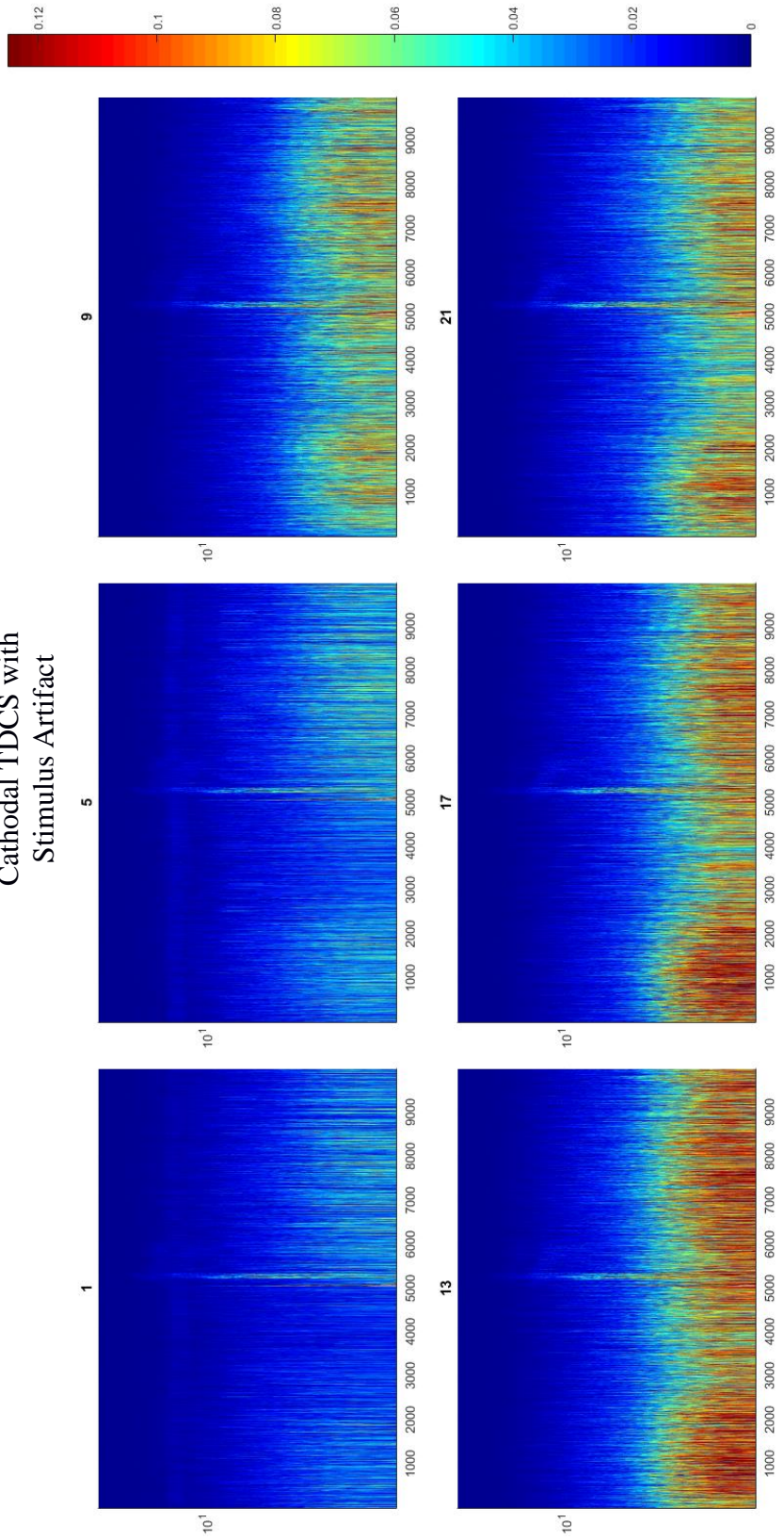


**Figure 13. Multi-taper estimate spectrograms representing the average power spectral density over time of the group of animals receiving cathodal TDCS and exhibiting stimulus artifact.** For each spectrogram the abscissa denotes time in number of moving window steps and the ordinate axis denotes frequency from 1-32 Hz on a logarithmic scale. Each moving window step corresponds to 0.3 seconds of actual recording time. Each spectrogram represents data from ten recordings concatenated in time. Color indicates normalized mean power.

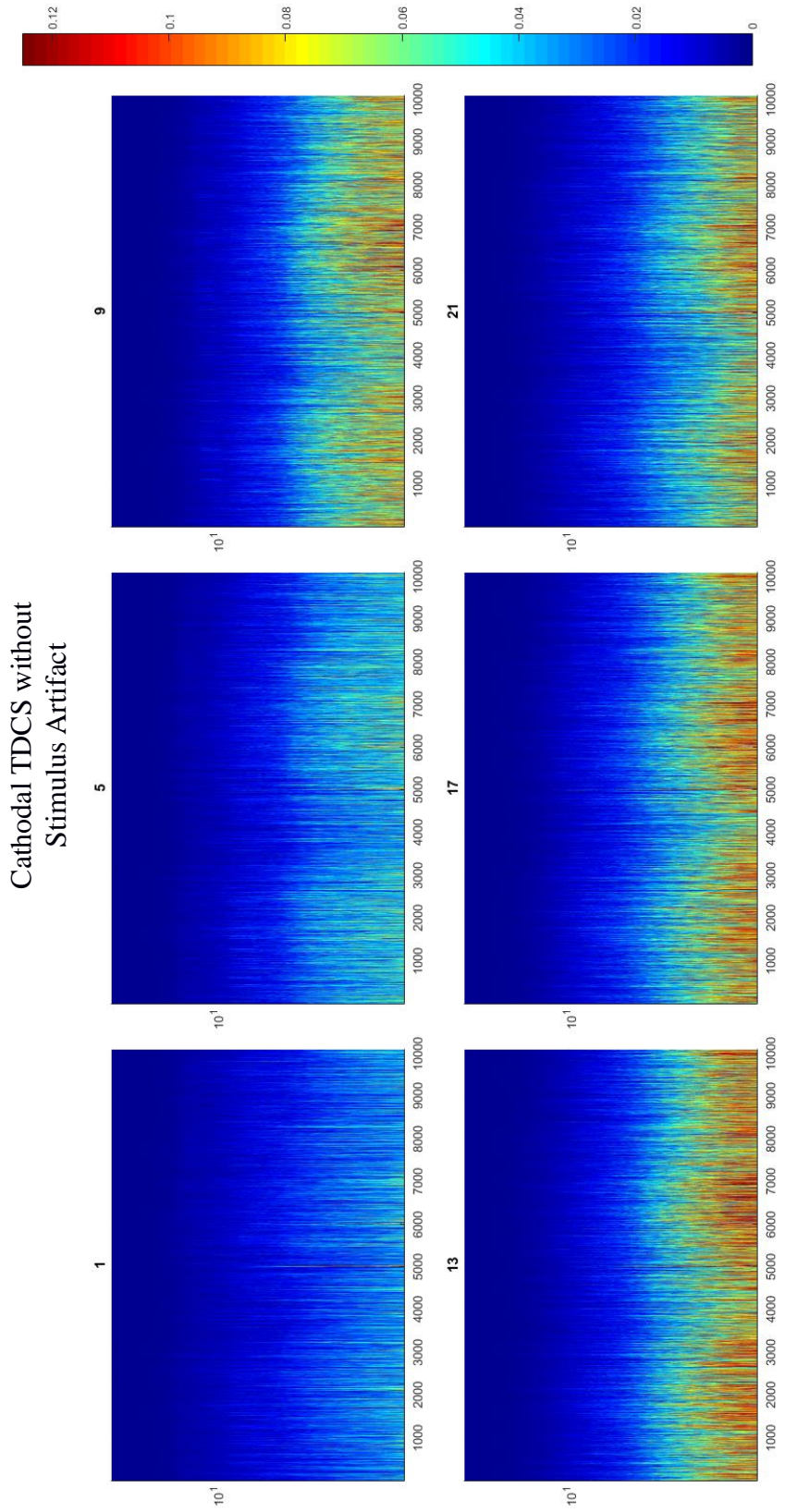


**Figure 14. Multi-taper estimate spectrograms representing the average power spectral density over time of the group of animals receiving cathodal TDCS without exhibiting stimulus artifact.** For each spectrogram the abscissa denotes time in number of moving window steps and the ordinate axis denotes frequency from 1-32 Hz on a logarithmic scale. Each moving window step corresponds to 0.3 seconds of actual recording time. Each spectrogram represents data from ten recordings concatenated in time. Color indicates normalized mean power.

## ***The Effect of TDCS on Cortical Spreading Depression Events***

### *Segregation and Refinement of Groups*

Animals were divided into groups similar to those used of the analysis of baseline activity, based on type of stimulation and presence of stimulus artifact. Assessment of stimulus artifact was based on presence or absence concurrent with stimulation during the fourth recording block. These groups were refined by removing animals that did not exhibit a CoSD event in the first five minutes of recording after the administration of KCl in the third recording block. Five animals, all having received anodal stimulation, were excluded from analysis for this reason. This resulted in group sizes as follows: anodal with stimulus artifact, n = 5; anodal without stimulus artifact, n = 3; cathodal with stimulus artifact, n = 7; cathodal without stimulus artifact, n = 4.

### *Outcome Assessment*

The outcome measure assessed was the presence or absence of spreading depression events occurring during the TDCS treatment period after administration of KCl. The results for each group are shown in Table 1.

Treatment group	Number of animals	Number of animals exhibiting CoSD event during TDCS	Percent of animals exhibiting CoSD event during TDCS
Anodal TDCS with stimulus artifact	5	2	40%
Anodal TDCS w/o stimulus artifact	3	2	67%
Cathodal TDCS with stimulus artifact	7	1	14%
Cathodal TDCS w/o stimulus artifact	4	3	75%

**Table 1. Results from assessment of the presence of CoSD events during the period of TDCS.**

### ***Transient Changes in Cortical Activity During CoSD Events***

Some recording data were processed into MTE spectrograms to explore the frequency-time representation of CoSD. The last recordings from the second block and the first recordings from the third block from four animals, during which the KCl induced CoSD event could be observed, were extracted and analyzed. These recordings underwent spectrogram processing, and for each animal, the second block recording was used as a baseline to normalize the third block recording. Spectrogram processing was similar to methods employed in previous analyses in this study, but with smaller moving window and step sizes (0.5 and 0.05 seconds respectively). This allowed for increased temporal resolution at the price of reduced frequency resolution. Normalization was done separately by channel and by frequency in order to better visualize minute power changes at higher frequencies.

For each set of recordings looked at in this way, CoSD events were observed on spectrograms as an extended period of heightened low frequency power. The



characteristic CoSD EEG wave synced up temporally with the duration of the low frequency activation. In addition, gamma band activation, from about 100-200 Hz, was observed to occur synchronously with the peak of the TDCS wave in each case analyzed (Figures 15A and 15B).

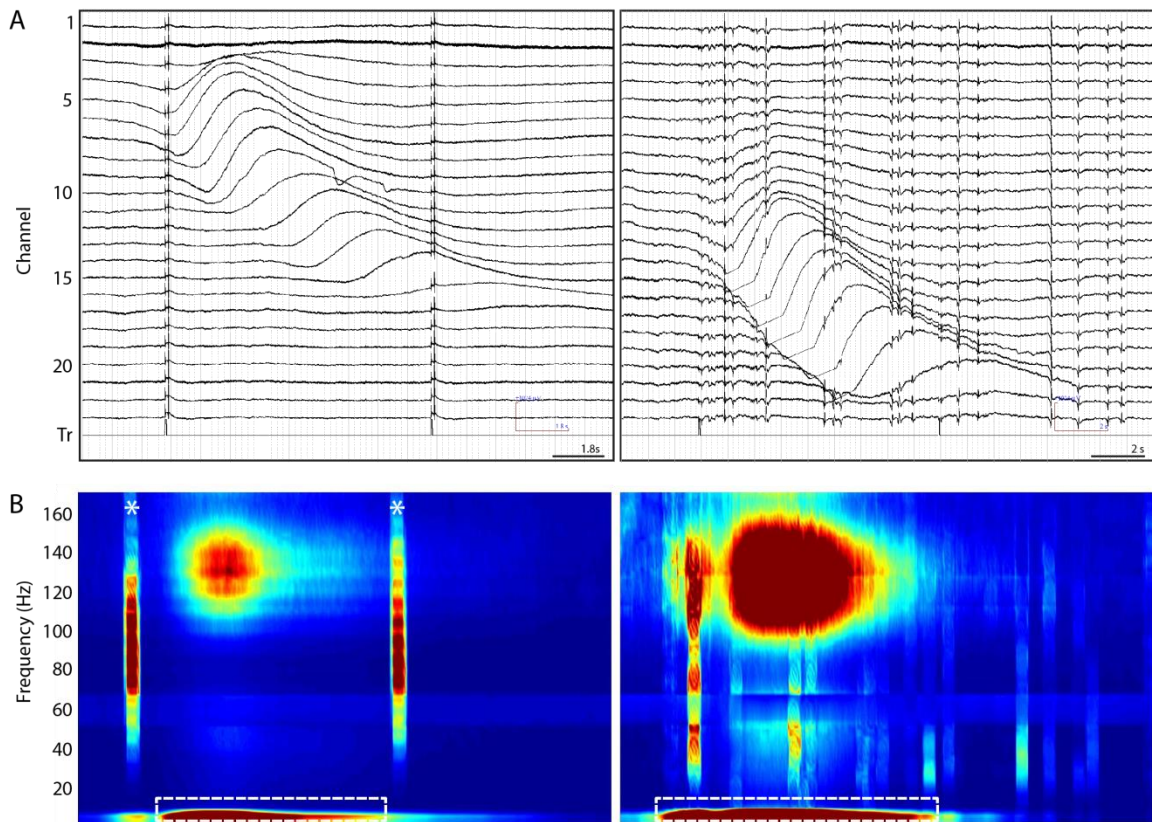


**Figure 15A. EEG recordings of CoSD events.** Separate cases from two different animals are displayed. **Figure 15B. Spectrograms of EEG recordings of CoSD events.** Each spectrogram shown below a given EEG trace has been generated from that EEG data and represents an average across channels affected by the CoSD event wave in the EEG trace. Warmer colors indicate higher normalized power. For each plot, the abscissa represents time and has been roughly synchronized with the time axis of its respective EEG trace. Increases in low frequency activity (outlined in the dashed white boxes) are observed to coincide with the characteristic CoSD event wave on the EEG. The peak of the EEG wave is further observed to occur synchronously with a burst of high frequency activity. The two time isolated bands of activity observed in the first spectrogram (marked \*) are artifacts of paired pulse stimulation in the contralateral hemisphere and are not related to CoSD activity.

Both the characteristic low and high frequency spectrogram signals observed to be associated with CoSD were only exhibited in recording channels that were affected by the CoSD wave on the corresponding EEG trace (Figure 16).

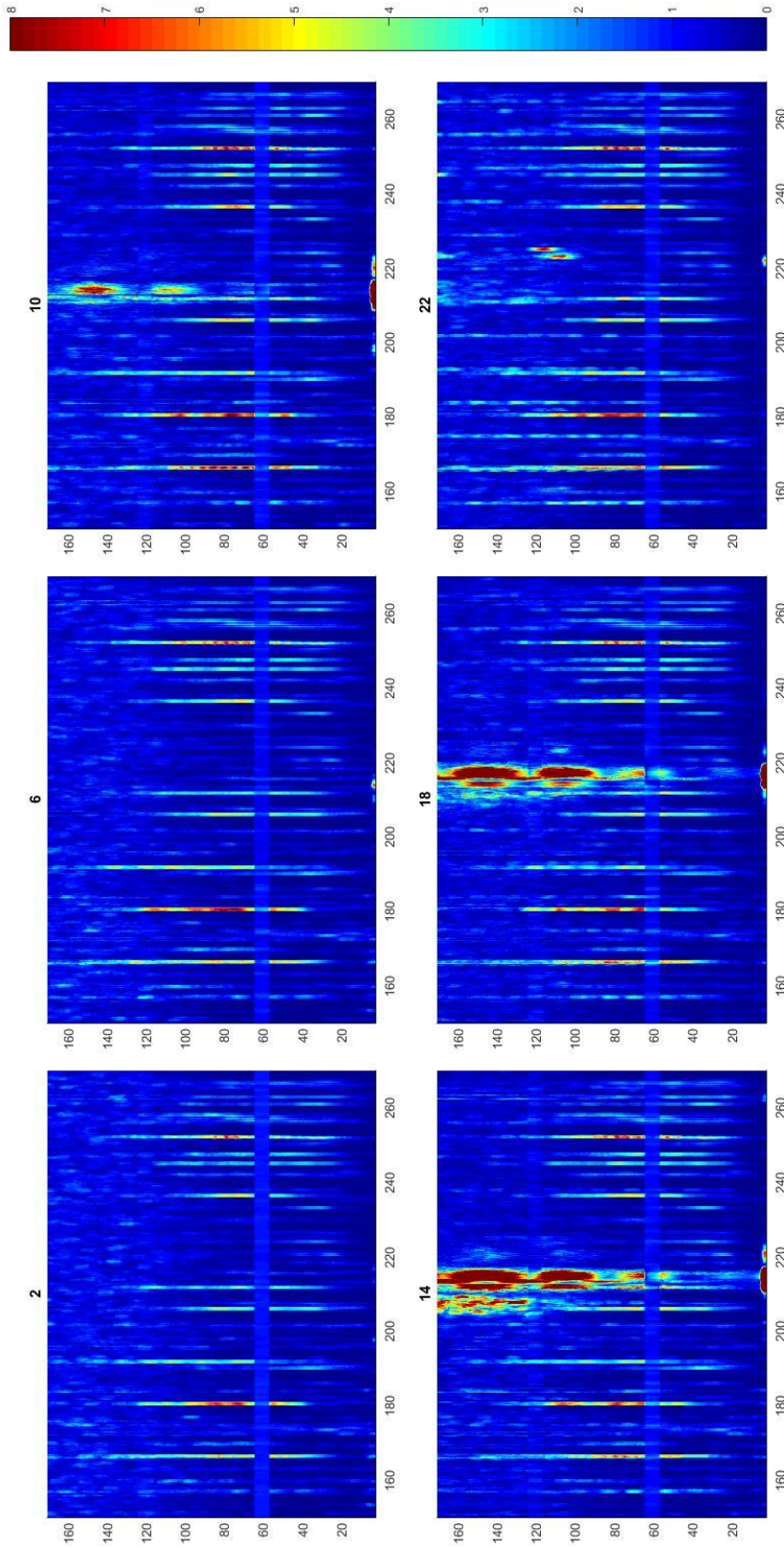


**Figure 16. Spectrograms demonstrating localization of CoSD event related gamma activation across channels.** These spectrogram data correspond to an EEG recording during which a CoSD event wave was observed to occur between recording channels 8 and 21 (see Figure 15A right). For each subplot, the abscissa represents time in seconds and the ordinate represents frequency in Hz. The color scale denotes power normalized to baseline by frequency. Each subplot presents the data from a separate channel. A spike in gamma activity can be observed during the CoSD event (at around 210 seconds) localized to the channels exhibiting CoSD wave activity on the EEG.

## DISCUSSION

The major findings of this study are as follows:

1. Anodal TDCS results in salient increases in delta and theta frequency activity in the rat cortex that last for 5 minutes on average after the end of stimulation.
2. Cathodal TDCS may inhibit the occurrence of CoSD events during the period of active stimulation, during which a stimulus artifact is present.
3. The CoSD event is accompanied by a burst of activity in the gamma band.
4. The presence or absence of TDCS stimulus artifact, as characterized by an increase in beta and/or alpha frequency activity strictly during the period of stimulation, can be used as a proxy for TDCS activity.

### *Anodal TDCS Amplifies Baseline Delta and Theta Band Activity*

This finding correlates fairly well with the findings of Mangia et al. (2014). However Mangia et al. report that anodal TDCS increased theta activity only for the duration of stimulation. However, our results appear to demonstrate elevation in both delta and theta band activity for several minutes beyond the period of active stimulation.

Although the salient effect and fairly low error from averaging within treatment groups is convincing, this study did not conduct formal statistical assessment of the significance of these results due to time restrictions. Future studies would seek to increase the animal number, perform formal sham experiments, and include formal significance measures.



### ***Cathodal TDCS Inhibits Occurrence of CoSD Events***

The treatment group receiving cathodal TDCS with stimulus artifact exhibited the lowest proportion of CoSD events during stimulation by a significant margin. However, the number of animals overall and per group is quite low, with the cathodal with stimulus artifact group having the most animals. It is therefore difficult to draw any firm conclusions. However, this provides a useful jumping off point for future studies seeking to incorporate the CoSD event as a correlate of CoSD. It is clear from these studies that more work needs to be done on the nature of the CoSD event and its role in the initiation or propagation of cortical spreading depression.

### ***The CoSD Event Occurs Concurrently with a Burst of Gamma Activity***

The observation that the peak of the CoSD wave on EEG recordings is always accompanied by a burst in gamma band activity is an unexpected finding of this study that could prove valuable in interpreting the nature of the CoSD event. This element of the CoSD phenomenon must be further verified and characterized to determine how, if indeed it does, fit within existing models of CoSD propagation, such as that described by Broberg et al. (2014).

### ***TDCS Stimulus Artifact Presence Is a Useful Proxy for TDCS Dosage***

One of the more distinguishing features of this study is the way that treatment groups were isolated. Instead of using formal shams, TDCS treated animals were

partitioned based on the presence or absence of an alpha/beta band stimulation artifact throughout treatment. Given the striking and consistent lack of effect of TDCS without stimulus artifact, both anodal and cathodal, it appears that stimulus artifact may in fact be a useful proxy for successful TDCS dosage. As discussed by Horvath et al. (2014), inter-subject variability in response to TDCS is a major issue in developing the technology towards clinical ends. Measures of successful TDCS treatment frequently vary wildly between groups for no apparent reason. Part of the problem is that TDCS by its nature as a non-invasive treatment is inexact and we do not currently have a reliable metric of successful dosage aside from treatment outcome measures. It is therefore intriguing that we have identified an independent measure which turns “on” and “off” in response to TDCS treatment, demonstrates intensity dependent on the intensity of stimulation, and which is associated with effective administration of TDCS.

### ***Conclusion***

This study reflects continuing advancement in the understanding of TDCS as a treatment modality, and as a scientific phenomenon. By demonstrating that anodal TDCS produces a lasting change in cortical activity in the delta and theta frequency bands, we have bolstered the current understanding of TDCS as a treatment that produces real changes in cortical activity that cannot simply be chalked up to the transient effect of the applied electrical current.

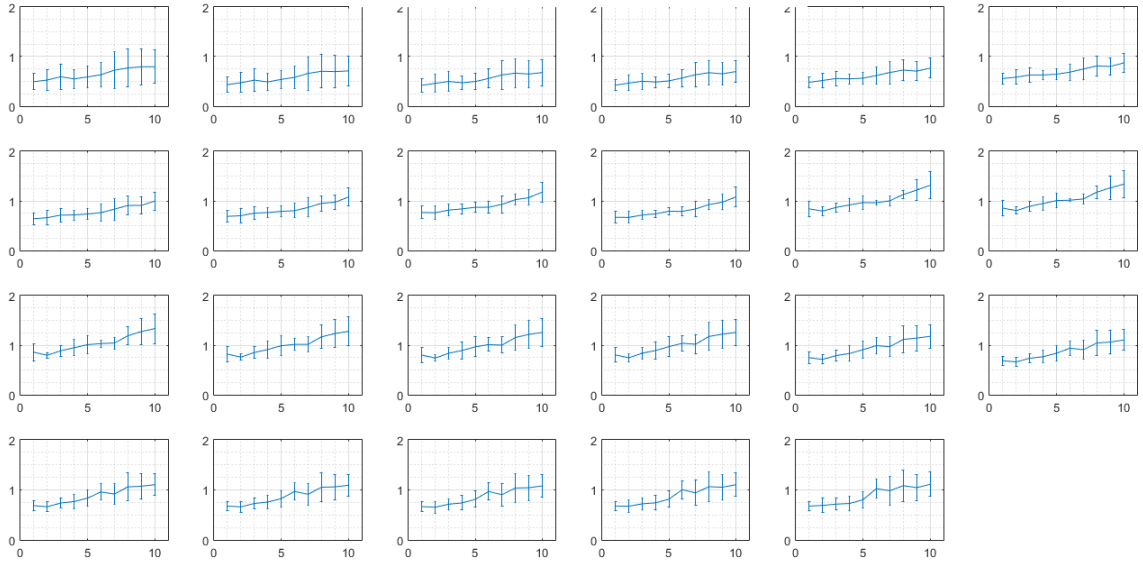
The result linking cathodal TDCS to the reduction of CoSD event occurrence lends further credence to TDCS as a possible non-invasive treatment for acute stroke or

other medical illnesses or conditions in which CoSD is implicated. The true implications of this finding depend on future studies elucidating the way in which the CoSD event fits into the puzzle of the CoSD phenomenon. We propose the burst in gamma activity observed to occur during the CoSD event as a promising subject for such future research.

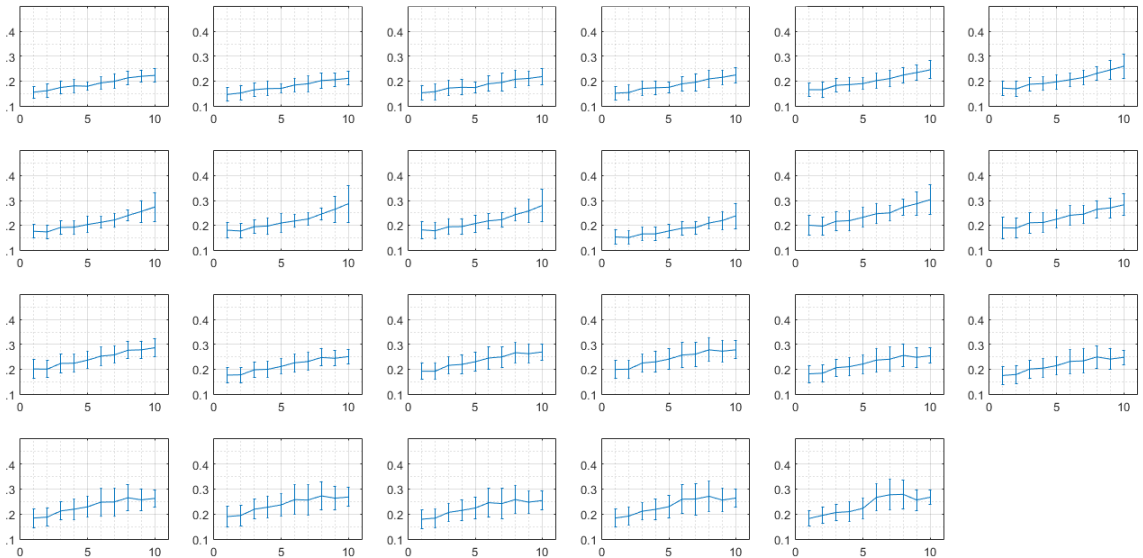
In conclusion, these results suggest that the alpha/beta frequency stimulus artifact be considered as a possible proxy measure of TDCS dosing. Of course, the true nature of the stimulus artifact and its relation to the mechanism of TDCS, as well as its predictive reliability in humans, must first be assessed thoroughly.

## APPENDIX A

### Anodal TDCS without Stimulus Artifact: Delta

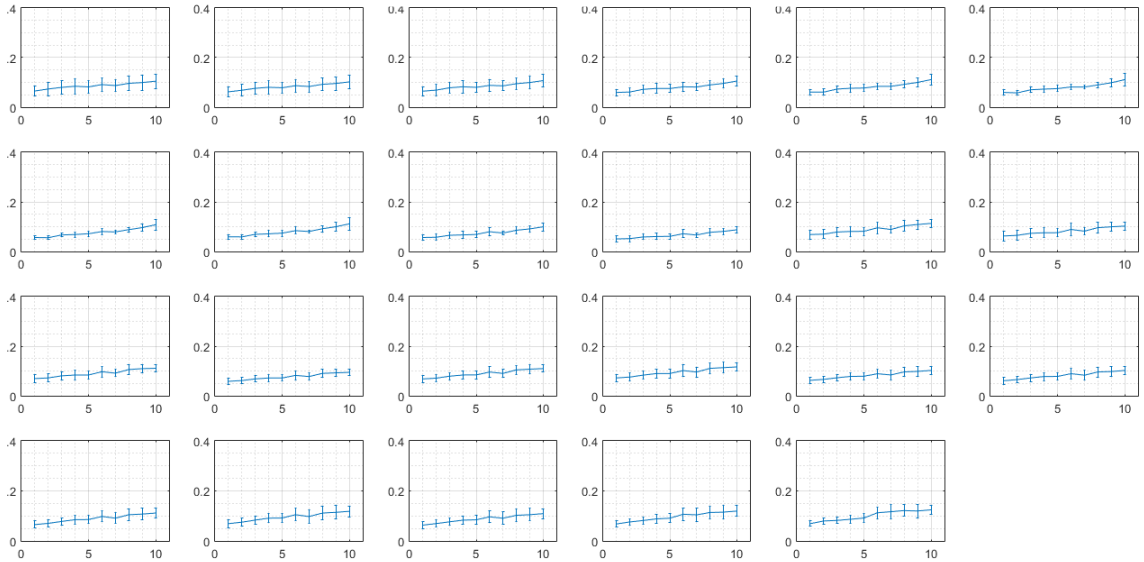


### Anodal TDCS without Stimulus Artifact: Theta

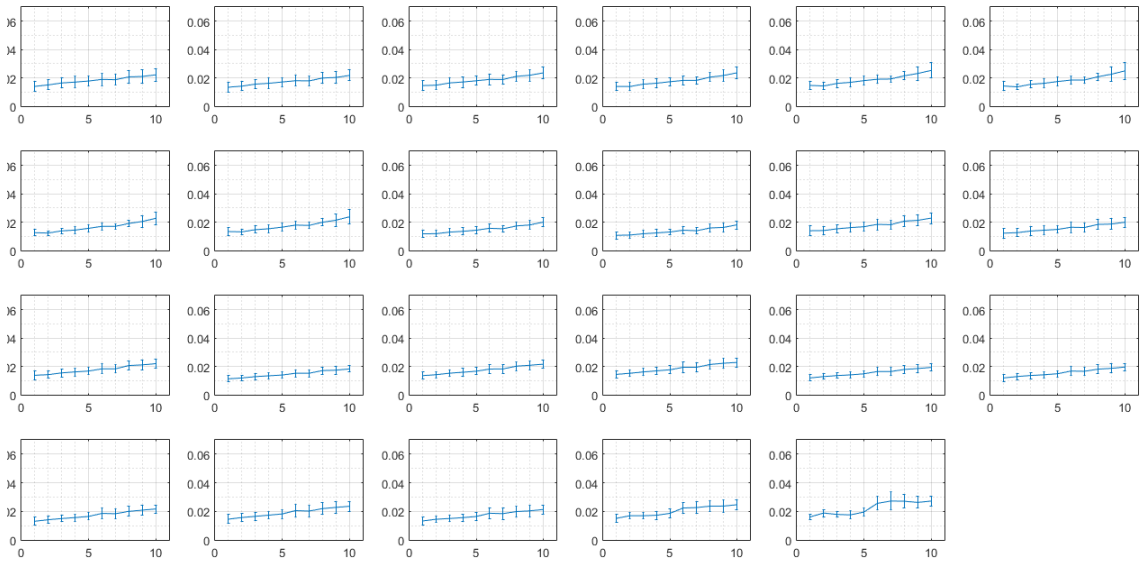


**Appendix A1. Plots displaying the average power spectral density in the delta and theta frequency bands by recording for the treatment group receiving anodal TDCS without demonstrating stimulus artifact. TDCS was administered throughout the 6<sup>th</sup> recording. Subplots are as described in Figure 5.**

Anodal TDCS without Stimulus  
Artifact: Alpha

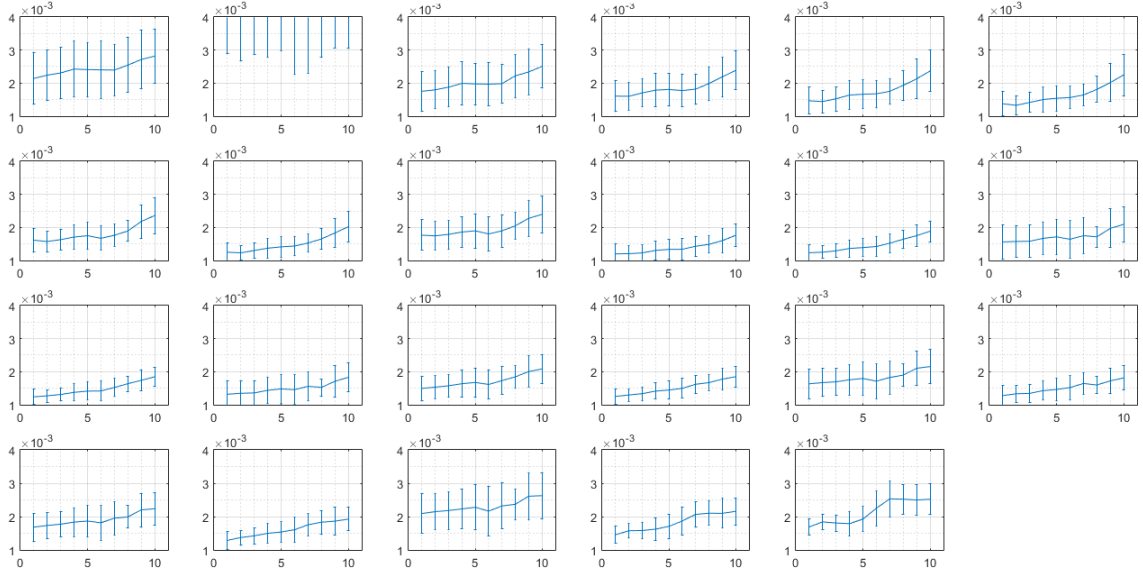


Anodal TDCS without Stimulus  
Artifact: Beta

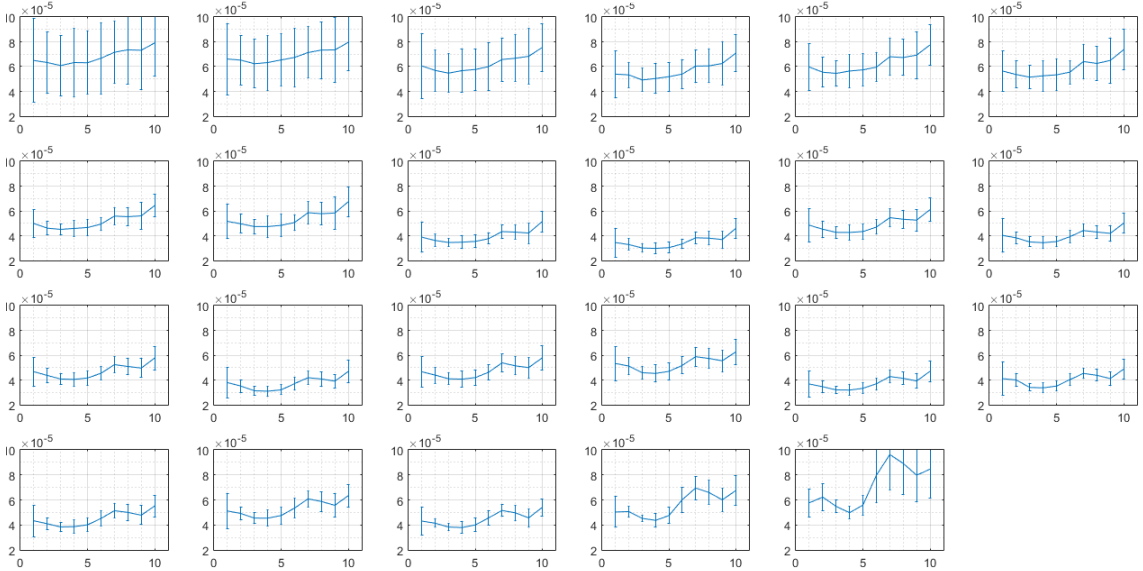


**Appendix A2. Plots displaying the average power spectral density in the alpha and beta frequency bands by recording for the treatment group receiving anodal TDCS without demonstrating stimulus artifact.** TDCS was administered throughout the 6<sup>th</sup> recording. Subplots are as described in Figure 5.

Anodal TDCS without Stimulus  
Artifact: Low Gamma



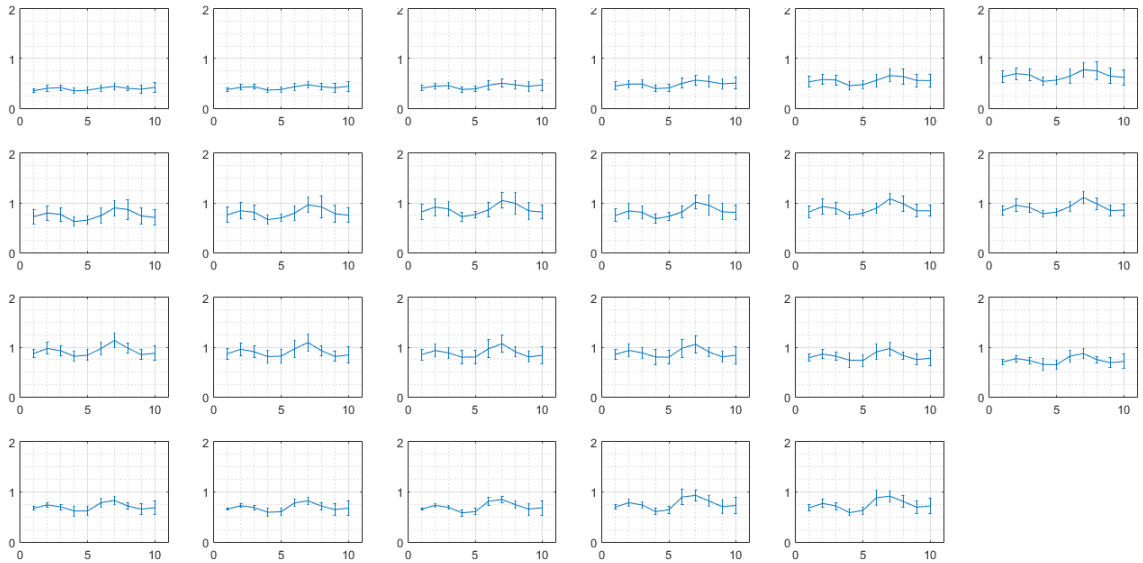
Anodal TDCS without Stimulus  
Artifact: High Gamma



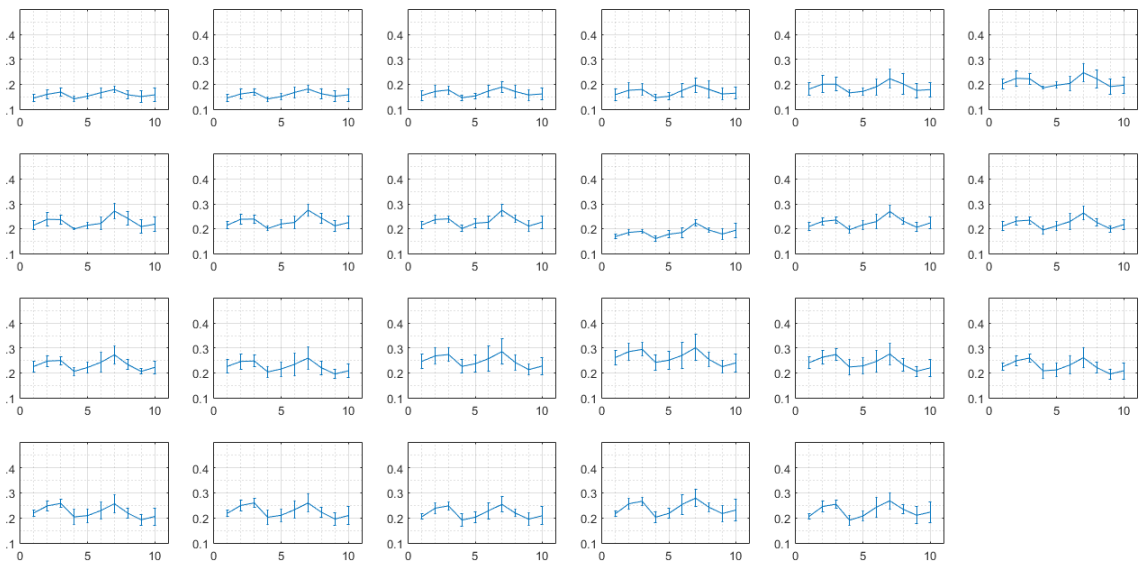
**Appendix A3. Plots displaying the average power spectral density in the low and high gamma frequency bands by recording for the treatment group receiving anodal TDCS without demonstrating stimulus artifact. TDCS was administered throughout the 6<sup>th</sup> recording. Subplots are as described in Figure 5.**

## APPENDIX B

### Cathodal TDCS without Stimulus Artifact: Delta

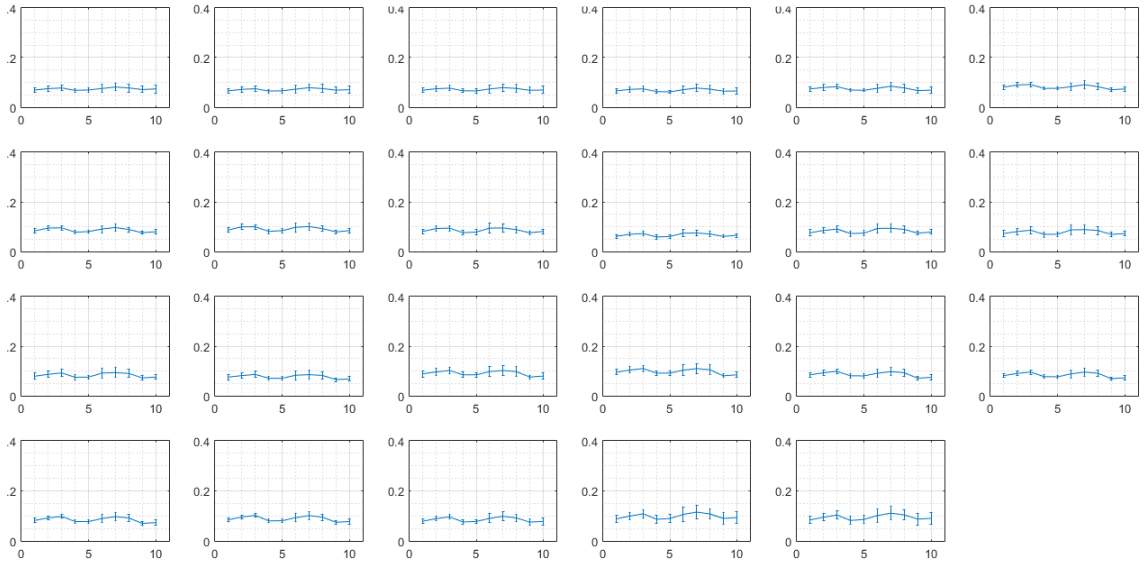


### Cathodal TDCS without Stimulus Artifact: Theta

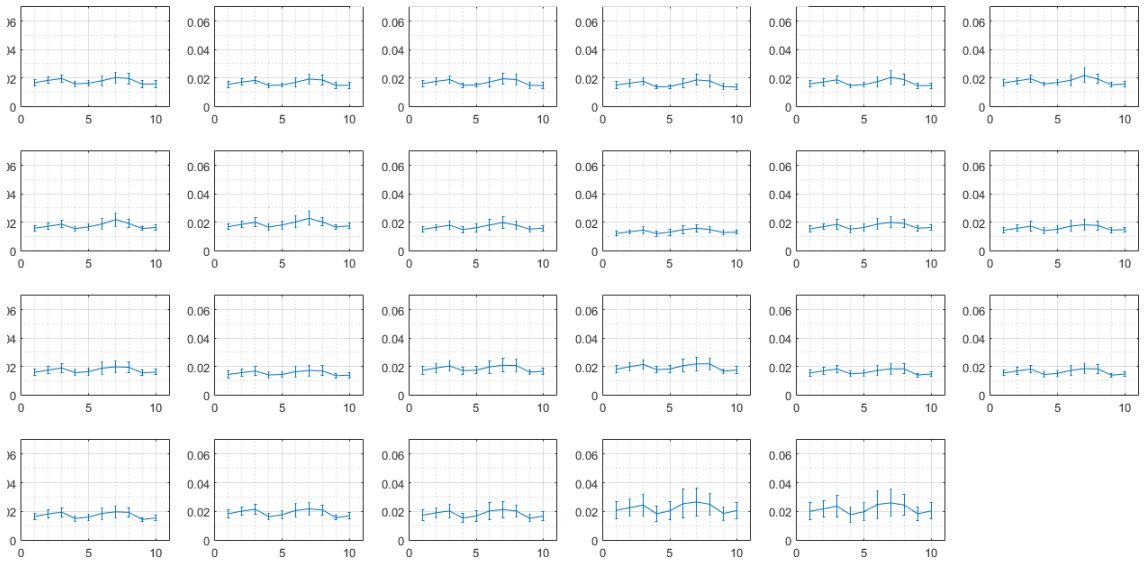


**Appendix B1.** Plots displaying the average power spectral density in the delta and theta frequency bands by recording for the treatment group receiving cathodal TDCS without demonstrating stimulus artifact. TDCS was administered throughout the 6<sup>th</sup> recording. Subplots are as described in Figure 5.

Cathodal TDCS without  
Stimulus Artifact: Alpha



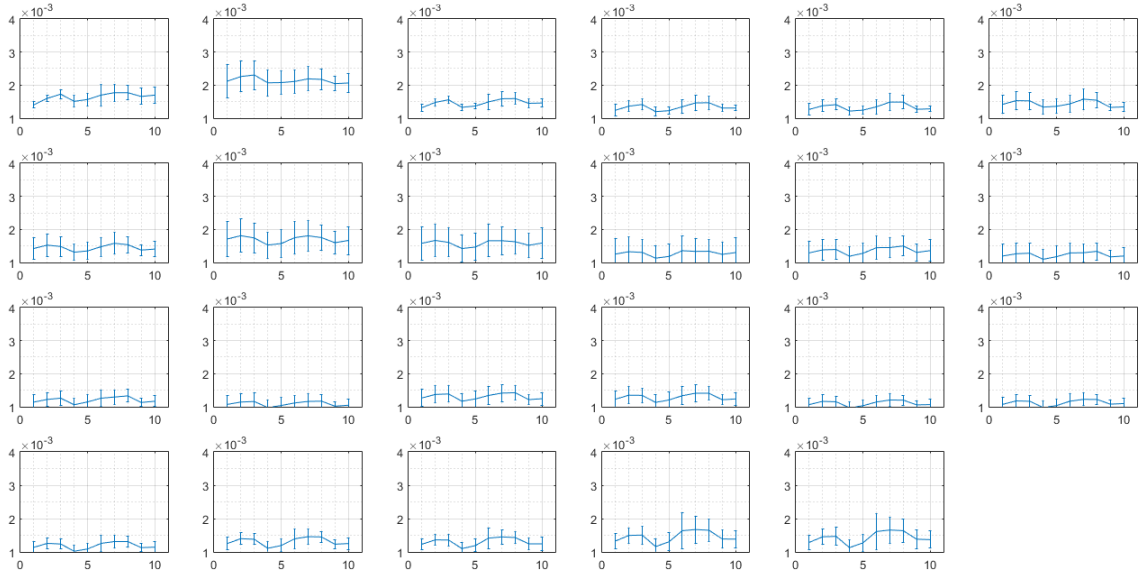
Cathodal TDCS without  
Stimulus Artifact: Beta



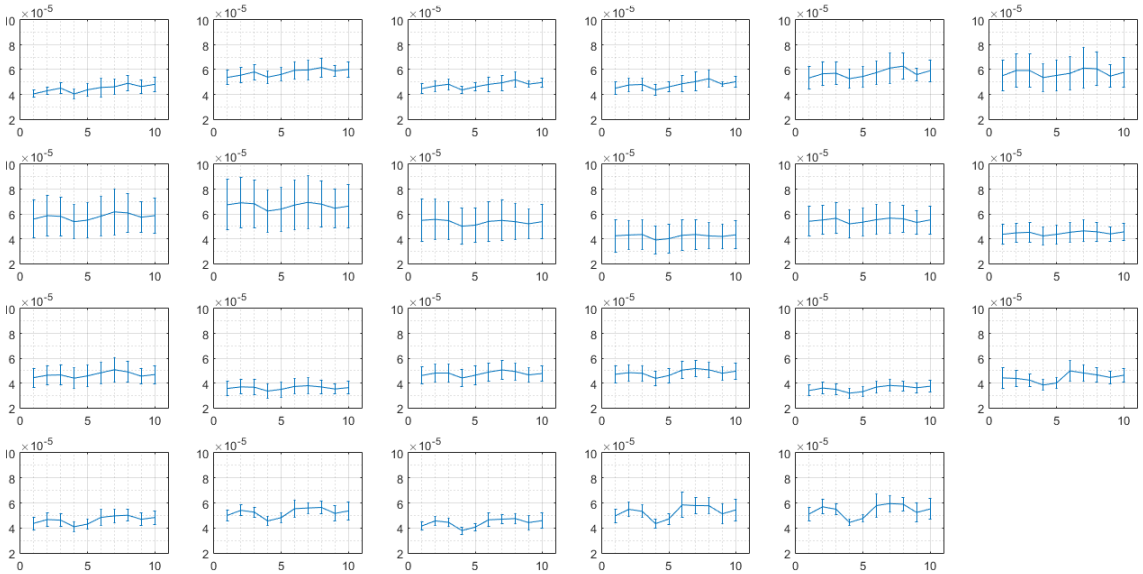
**Appendix B2. Plots displaying the average power spectral density in the alpha and beta frequency bands by recording for the treatment group receiving cathodal TDCS without demonstrating stimulus artifact. TDCS was administered throughout the 6<sup>th</sup> recording. Subplots are as described in Figure 5.**



Cathodal TDCS without  
Stimulus Artifact: Low Gamma



Cathodal TDCS without  
Stimulus Artifact: High Gamma



**Appendix B3. Plots displaying the average power spectral density in the low and high gamma frequency bands by recording for the treatment group receiving cathodal TDCS without demonstrating stimulus artifact. TDCS was administered throughout the 6<sup>th</sup> recording. Subplots are as described in Figure 5.**

## REFERENCES

- Accornero, N., Capozza, M., Pieroni, L., Pro, S., Davì, L., & Mecarelli, O. (2014). EEG mean frequency changes in healthy subjects during prefrontal transcranial direct current stimulation. *Journal of Neurophysiology*, *112*(6), 1367–1375. <http://doi.org/10.1152/jn.00088.2014>
- Aiba, I., & Shuttleworth, C. W. (2012). Sustained NMDA receptor activation by spreading depolarizations can initiate excitotoxic injury in metabolically compromised neurons. *The Journal of Physiology*, *590*(Pt 22), 5877–5893. <http://doi.org/10.1113/jphysiol.2012.234476>
- Bindman, L. J., Lippold, O. C. J., & Redfearn, J. W. T. (1964). The action of brief polarizing currents on the cerebral cortex of the rat (1) during current flow and (2) in the production of long-lasting after-effects. *The Journal of Physiology*, *172*(3), 369.
- Bokil, H., Andrews, P., Kulkarni, J. E., Mehta, S., & Mitra, P. (2010). Chronux: A Platform for Analyzing Neural Signals. *Journal of Neuroscience Methods*, *192*(1), 146–151. <http://doi.org/10.1016/j.jneumeth.2010.06.020>
- Broberg, M., Pope, K. J., Olsson, T., Shuttleworth, C. W., & Willoughby, J. O. (2014). Spreading depression: Evidence of five electroencephalogram phases. *Journal of Neuroscience Research*, *92*(10), 1384–1394. <http://doi.org/10.1002/jnr.23412>
- Broeder, S., Nackaerts, E., Heremans, E., Vervoort, G., Meesen, R., Verheyden, G., & Nieuwboer, A. (2015). Transcranial direct current stimulation in Parkinson's disease: Neurophysiological mechanisms and behavioral effects. *Neuroscience & Biobehavioral Reviews*, *57*, 105–117. <http://doi.org/10.1016/j.neubiorev.2015.08.010>
- Dhamne, S. C., Ekstein, D., Zhuo, Z., Gersner, R., Zurakowski, D., Loddenkemper, T., ... Rotenberg, A. (2015). Acute seizure suppression by transcranial direct current stimulation in rats. *Annals of Clinical and Translational Neurology*, *2*(8), 843–856. <http://doi.org/10.1002/acn3.226>
- Dohmen, C., Sakowitz, O. W., Fabricius, M., Bosche, B., Reithmeier, T., Ernestus, R.-I., ... Graf, R. (2008). Spreading depolarizations occur in human ischemic stroke with high incidence. *Annals of Neurology*, *63*(6), 720–728. <http://doi.org/10.1002/ana.21390>
- Dreier, J. P. (2011). The role of spreading depression, spreading depolarization and spreading ischemia in neurological disease. *Nature Medicine*, *17*(4), 439–447. <http://doi.org/10.1038/nm.2333>

- Dubljević, V., Saigle, V., & Racine, E. (2014). The Rising Tide of tDCS in the Media and Academic Literature. *Neuron*, 82(4), 731–736. <http://doi.org/10.1016/j.neuron.2014.05.003>
- Enger, R., Tang, W., Vindedal, G. F., Jensen, V., Helm, P. J., Sprengel, R., ... Nagelhus, E. A. (2015). Dynamics of Ionic Shifts in Cortical Spreading Depression. *Cerebral Cortex*, 25(11), 4469–4476. <http://doi.org/10.1093/cercor/bhv054>
- Fertonani, A., & Miniussi, C. (2016). Transcranial Electrical Stimulation What We Know and Do Not Know About Mechanisms. *The Neuroscientist*, 1073858416631966. <http://doi.org/10.1177/1073858416631966>
- Fritsch, B., Reis, J., Martinowich, K., Schambra, H. M., Ji, Y., Cohen, L. G., & Lu, B. (2010). Direct current stimulation promotes BDNF-dependent synaptic plasticity: Potential implications for motor learning. *Neuron*, 66(2), 198–204. <http://doi.org/10.1016/j.neuron.2010.03.035>
- Horvath, J. C., Carter, O., & Forte, J. D. (2014). Transcranial direct current stimulation: five important issues we aren't discussing (but probably should be). *Frontiers in Systems Neuroscience*, 8. <http://doi.org/10.3389/fnsys.2014.00002>
- Hoy, K. E., Bailey, N. W., Arnold, S. L., & Fitzgerald, P. B. (2015). The effect of transcranial Direct Current Stimulation on gamma activity and working memory in schizophrenia. *Psychiatry Research*, 228(2), 191–196. <http://doi.org/10.1016/j.psychres.2015.04.032>
- Knotkova, H., Nitsche, M. A., & Cruciani, R. A. (2013). Putative physiological mechanisms underlying tDCS analgesic effects. *Frontiers in Human Neuroscience*, 7. <http://doi.org/10.3389/fnhum.2013.00628>
- Liebetanz, D., Fregni, F., Monte-Silva, K. K., Oliveira, M. B., Amâncio-dos-Santos, Â., Nitsche, M. A., & Guedes, R. C. A. (2006). After-effects of transcranial direct current stimulation (tDCS) on cortical spreading depression. *Neuroscience Letters*, 398(1–2), 85–90. <http://doi.org/10.1016/j.neulet.2005.12.058>
- López-Alonso, V., Cheeran, B., Río-Rodríguez, D., & Fernández-del-Olmo, M. (2014). Inter-individual Variability in Response to Non-invasive Brain Stimulation Paradigms. *Brain Stimulation*, 7(3), 372–380. <http://doi.org/10.1016/j.brs.2014.02.004>
- Mangia, A. L., Pirini, M., & Cappello, A. (2014). Transcranial direct current stimulation and power spectral parameters: a tDCS/EEG co-registration study. *Frontiers in Human Neuroscience*, 8. <http://doi.org/10.3389/fnhum.2014.00601>

- Miller, J., Berger, B., & Sauseng, P. (2015). Anodal transcranial direct current stimulation (tDCS) increases frontal–midline theta activity in the human EEG: A preliminary investigation of non-invasive stimulation. *Neuroscience Letters*, 588, 114–119. <http://doi.org/10.1016/j.neulet.2015.01.014>
- Nakamura, H., Strong, A. J., Dohmen, C., Sakowitz, O. W., Vollmar, S., Sué, M., ... Graf, R. (2010). Spreading depolarizations cycle around and enlarge focal ischaemic brain lesions. *Brain*, 133(7), 1994–2006. <http://doi.org/10.1093/brain/awq117>
- Nitsche, M. A., Fricke, K., Henschke, U., Schlitterlau, A., Liebetanz, D., Lang, N., ... Paulus, W. (2003). Pharmacological Modulation of Cortical Excitability Shifts Induced by Transcranial Direct Current Stimulation in Humans. *The Journal of Physiology*, 553(1), 293–301. <http://doi.org/10.1113/jphysiol.2003.049916>
- Nitsche, M. A., & Paulus, W. (2000). Excitability changes induced in the human motor cortex by weak transcranial direct current stimulation. *The Journal of Physiology*, 527(Pt 3), 633–639. <http://doi.org/10.1111/j.1469-7793.2000.t01-1-00633.x>
- Notturmo, F., Pace, M., Zappasodi, F., Cam, E., Bassetti, C. L., & Uncini, A. (2014). Neuroprotective effect of cathodal transcranial direct current stimulation in a rat stroke model. *Journal of the Neurological Sciences*, 342(1–2), 146–151. <http://doi.org/10.1016/j.jns.2014.05.017>
- Ruffini, G., Wendling, F., Merlet, I., Molaee-Ardekani, B., Mekonnen, A., Salvador, R., ... Miranda, P. C. (2013). Transcranial Current Brain Stimulation (tCS): Models and Technologies. *IEEE Transactions on Neural Systems and Rehabilitation Engineering*, 21(3), 333–345. <http://doi.org/10.1109/TNSRE.2012.2200046>
- Song, M., Shin, Y., & Yun, K. (2014). Beta-frequency EEG activity increased during transcranial direct current stimulation: *NeuroReport*, 25(18), 1433–1436. <http://doi.org/10.1097/WNR.0000000000000283>
- Stagg, C. J., & Johansen-Berg, H. (2013). Studying the Effects of Transcranial Direct-Current Stimulation in Stroke Recovery Using Magnetic Resonance Imaging. *Frontiers in Human Neuroscience*, 7. <http://doi.org/10.3389/fnhum.2013.00857>
- Strong, A. J., Anderson, P. J., Watts, H. R., Virley, D. J., Lloyd, A., Irving, E. A., ... Graf, R. (2007). Peri-infarct depolarizations lead to loss of perfusion in ischaemic gyrencephalic cerebral cortex. *Brain*, 130(4), 995–1008. <http://doi.org/10.1093/brain/awl392>

## CURRICULUM VITAE

### ANDREW STANFORD CHANG

**Year Born:** 1991

**Address:** 775 Tremont Street, Apt. 1R, Boston, MA 02118

**Phone:** (408) 806-8085

**Email:** andrew.stf.chang@gmail.com

#### Education

Boston University School of Medicine

**Master of Science in Medical Sciences**

August 2014- Present

Concentration in Mental Health Counseling and Behavioral Medicine

University of California, Berkeley

**Bachelor of Arts in Molecular and Cell Biology**

August 2009- May 2013

Emphasis in Neurobiology, Minor in Chemistry

#### Employment and Experience

Medimmune LLC, Mountain View, CA

**Research Associate, Virology Group**

June 2013- March 2014

- Independently pursued and completed project with goal of expressing several viral proteins in eukaryotic cell culture and subsequent purification and quantitation of product for antiserum generation.
- Seasonal flu vaccine strain selection involving wild type strain gene analysis, viral gene cloning, and rescue and characterization of cold adapted vaccine strains.

Harland Lab of Genomics and Development, U.C. Berkeley, CA

**Undergraduate Research Assistant**

August 2011- May 2012

- Reverse genetics experimentation in the model organisms *Xenopus laevis* and *Xenopus tropicalis* studying signaling mechanisms behind neural crest induction in vertebrates.
- Carried out day to day experimental procedures required for molecular cloning, morpholino RNA transcript knockdown, and in situ hybridization.

Silver Lab of Visual Neuroscience, U.C. Berkeley, CA

**Undergraduate Research Assistant**

January 2011- May 2011

- Recruitment of subjects for a research study analyzing the potential effects of an on-market neurotransmitter agonist on peripheral visual acuity.

- Management of multiple time-sensitive experimental trials per subject over several weeks.
- Recording and organization of experimental data on a computer database and maintenance of subject pool database.

### **Activities**

Suitcase Clinic, Berkeley, CA

#### **Community Resources Coordinator**

August 2010- May 2013

- Maintenance of database of local medical, dental, and psychiatric services for low income and homeless persons and referral of clinic clients to appropriate community resources and social services.